CHALMERS
UNIVERSITY OF TECHNOLOGY

Geometry Effects of Laser Tempering in Boron Steel before Self-Pierce Riveting

Master's Thesis in Product Development

SOFFÍA ARNÞRÚÐUR GUNNARSDÓTTIR
ALEJANDRO RODRÍGUEZ BASURTO

Geometry Effects of Laser Tempering in Boron Steel Before Self-Pierce Riveting

by

SOFFÍA ARNÞRÚÐUR GUNNARSDÓTTIR
ALEJANDRO RODRÍGUEZ BASURTO

Department of Product & Production Development
Division of Product Development
CHALMERS UNIVERSITY OF TECHNOLOGY

Gothenburg, Sweden 2015

Geometry Effects of Laser Tempering in Boron Steel before Self-Pierce Riveting
SOFFÍA ARNÞRÚÐUR GUNNARSDÓTTIR
ALEJANDRO RODRÍGUEZ BASURTO

Master Thesis 2015:06
Department of product & production development
CHALMERS UNIVERSITY OF TECHNOLOGY
SE-412 96 Göteborg
Sweden
Telephone + 46 (0) 31-772 1000

Cover:
XC90 Safety Cage, p. 7 (Volvo Cars, 2013)

Chalmers Reproservice
Gothenburg, Sweden 2015

Geometry Effects of Laser Tempering in Boron Steel before Self-Pierce Riveting
SOFFÍA ARNÞRÚÐUR GUNNARSDÓTTIR
ALEJANDRO RODRÍGUEZ BASURTO
Department of Product & Production Development
Division of Product Development
CHALMERS UNIVERSITY OF TECHNOLOGY

ABSTRACT

The automotive industry is asking for new ways to reduce the weight of their vehicles while keeping up to higher safety standards. In the request for new materials, boron steel represents a good option along with other materials that will allow the weight to be reduced. New ways to join these materials have to be developed, and this is where self-pierce riveting comes to play. Since boron steel is a very hard material, it has to be locally softened with a laser, which has been proven to deform the part. The deformation has an impact on the overall quality of the final assembly, reason for which it is of interest to study. The causes of the deformation are presented in this thesis through literature studies. Next, the optimal laser parameters are examined to meet the ideal hardness for self-pierce rivet. Right after, results from thermo-mechanical simulations in RD&T's newly developed Heat Analysis module are presented, proving the existence of a relation between sequence and deformation. A gap analysis of the software, regarding interface and functionality, is included. It finalises with discussion about the overall work, recommendations and conclusions.

Keywords: boron steel, laser tempering, self-pierce riveting, deformation, hardness, softening, RD&T, thermo-mechanical simulation.

PREFACE

This master thesis is proposed by the research group "Geometry Assurance and Robust Design" which works with tools and methods to reduce the effects of geometrical variation. This is done in cooperation with Swerea IVF and Volvo Car Corporation, as a contribution to a collaborative project called *PLUGG*.

ACKNOWLEDGEMENTS

During the time we spent writing our thesis work, we met wonderful people who was always eager to help us. We appreciate your time, support and patience; you made a big contribution to it.

Thanks to our supervisors at Chalmers, Kristina Wärmefjord and Rikard Söderberg; at Swerea IVF, Fredrik Wandebäck and Ola Albinsson; and at Volvo Cars, Stefan Hansson, who guided and supported this thesis in many ways.

Additional people were consulted all along this time, and also showed up to be super friendly and helpful to achieve what is presented now, we truly appreciate your support as well: Albin Stormvinter, Peter Ottosson, Hans Kristoffersen, Johan Ermstål Pilthammar, Kerstin Wasmuth, Mats Sigvant, Samuel C Lorin, and Lars Lindkvist. (Are we missing one? I hope we are not)

Of course this could not have been possible without the support of our loved ones, our family and friends. They were extraordinary supportive by cheering us up, company, listening to our frustrations, and bouncing back ideas. Some them did it while in Sweden, and some from our home countries, Iceland and Mexico. Guess who is from where. Thank you again.

Gothenburg, June 2015

Soffia A. Gunnarsdottir & Alejandro Rodríguez Basurto

LIST OF ACRONYMS

SPR	–	Self Pierce Riveting
VCC:	–	Volvo Car Corporation
AHSS	–	Advanced High Strength Steel
UHSS	–	Ultra High Strength Steel
RD&T	–	Robust Design and Tolerance
CAT	–	Computer Aided Translation
CAD	–	Computer Aided Design
USL	–	Upper Specification Limit
LSL	–	Lower Specification Limit
SPA	–	Scalable Product Architecture
TSP	–	Traveling Salesman Problem

CONTENTS

1 INTRODUCTION

1.1 Background and Motivation

The Swedish government and the automotive industry created the FFI program, which is a joint funding initiative for research, innovation and development focusing on environment, climate, and safety. The program concentrates on social goals regarding environment, energy and traffic safety, in combination with competitiveness and job creation in Sweden. It is two thirds focused on environmental impact and one third on safety improvement. Additional projects within production technology, new technologies and materials may be included as well (Vinnova, 2012).

The FFI project calls for an increased safety while reducing fuel consumption, forcing the automotive companies to create safer structures for the vehicles with reduced weight. Safety improvements in the vehicle come from the addition of active and passive safety systems, which represent a higher mass and thus higher CO2 emission. Additionally, the incursion of the electric and hybrid car requires the car structures to be lighter in order to compensate the weight increase from the batteries.

New lightweight materials have to be introduced in the car body to reduce weight. This means that the variation of materials increases and a new challenge arises by requiring a way to join materials with different properties. The joining methods become crucial in these complex assemblies. The problem is to find new ways to join these completely new materials and combinations since today's traditional joining technologies find it difficult, or in many cases, impossible to do.

Volvo Cars Corporation (VCC), a member of the FFI program, manufactures cars in the premium segment. Under this program, VCC together with Swerea IVF, have formed a project called "PLUGG". The purpose of the project is to develop a robust process for mechanical joining of non-compatible materials based on self-piercing riveting (SPR). Since the current base material for a VCC vehicle is steel, the transition to reduce weight is being made by extending the use of aluminium and composite materials, which are hardly possible to join with current techniques.

In an attempt to join different materials, one part of the PLUGG project is concerned about joining boron steel with composite materials. The proposed joining method is self-pierce riveting. The boron steel is a very hard material that needs to be softened before this process, so a part of this project is about laser point tempering of an A-Pillar made of boron steel before being self-pierce riveted. The part gets deformed when tempered, so this thesis work will attain to find the causes for this geometry variation, to find a relation between sequence and deformation, and to establish the laser parameters to meet SPR requirements. The variation tool RD&T is a software used to investigate that relation, followed by a comprehensive gap analysis of the software.

1.2 Research Goals and Objectives

The goal is to find a relation between deformation and sequence when laser tempering an A-pillar. The thesis goal will be delivered as:

1. Ranking of factors affecting geometrical impact for the case part.
2. Establish the laser parameters to get the optimal hardness for self-pierce riveting.
3. Define the relation between laser sequence and deformation.
4. Gap analysis of RD&T's Heat Analysis module.

1.3 Scope and Limitations

In this project the objective will be to find the causes for deformation, when an A-Pillar from a VCC vehicle (Figure 1) is tempered by using a laser. The part is made of boron steel Usibor® 1500, a registered trademark from ArcelorMittal. The laser tooling, and the parameters used during the process, will be researched in cooperation with Swerea IVF and VCC.

Figure 1: A-pillar

The study of sequences will only be developed with the case part in mind and with fixed process parameters. However, as part of the project, the method and conditions established will be discussed to see the possibility of using it as a universal method for other cases; other methods and conditions for alternative solutions will also be mentioned.

The main part of the study is the simulation process which will be performed with RD&T, theoretical support from existing literature, and expertise from employees at VCC and Swerea IVF. The Heat Analysis module in RD&T was required to be used in the thesis work for thermo-mechanical simulations. Since the laser parameters are crucial to obtain the adequate hardness on the material, they will be also considered as topics of study. No studies will be made on the processes before or after the laser tempering.

1.4 Method and Outline

For pursuing the thesis goals and its deliverables, the following tasks will be performed:

- **Literature studies of laser tempering in boron steel**: Information will be approached from literature such as books, scientific papers and reports. It will be divided into the following subjects:
  - Boron steel material properties.
  - Related manufacturing processes, e.g., hot stamping, heat treatments, laser tempering, and self-pierce riveting.
  - Heat effects on stamped sheet metal parts.
  - Selecting welding sequences, optimization techniques, and geometry assurance.
- **Consult experts to describe and analyse process parameters for tempering:** There is also knowledge that is not found in literature. The experts working in the manufacturing and assembly processes play an exceptional role in providing unwritten information. These people have years of experience in the field, and might know data to provide clues that can contribute to the study.
- **Laser and hardness testing:** The laser parameters are tested on coupons to find the necessary temperature to soften the material to the required hardness for SPR.
- **Modelling of a case, using the CAT-tool RD&T:** The CAD model will be received from VCC and imported into RD&T for analysis. The software will have a specially developed module for thermos-mechanical simulation, which will allow to predict the part behaviour when exposed to heat. Before the creation of the simulation model, the laser parameters have to be defined in order to make the right setup. Next, a physical verification of the geometrical impact is carried out. For this task, the simulation compared to the reality will provide a way to show the effectiveness of the method and of the software itself.
- **Gap study of needed functionality in the RD&T software:** The information from the literature and the experts will be complemented by data obtained from the use of RD&T. If RD&T misses relevant functionalities, it will be documented and revealed for further development of the software. The effectiveness of RD&T as a tool for predicting thermal impact on geometry will be also evaluated at this point.

The structure of the thesis is as follows. In Chapter 1, the background of the thesis is introduced along with its objectives. Next, the scope and limitations are outlined followed by the description of methods that will be used. Chapter 2 covers the literature study where the aim is to answer the first goal deliverable. Chapter 3 describes previous work done by Swerea and VCC, and includes the laser tests where the second goal deliverable is obtained. In Chapter 4, the relation between sequence and deformation is found, which is the third goal deliverable. The simulation process is described, including relevant findings for further tool development. Chapter 5 is the discussion, covering the thesis weaknesses, validity and difficulties. This is followed with chapter 6, recommendation of next steps and finally, the thesis work is summarized along with a conclusion in chapter 7.

2 LITERATURE REVIEW

2.1 Geometrical Variation, Geometry Assurance and RD&T

Geometrical variation in parts and assemblies in the automotive industry is a problem that affects the size, shape, and position of subassemblies or final products. This may cause problems when assembling the parts or the final products not meeting the functional and aesthetical requirements (Wärmefjord, 2004). All manufacturing processes have variation and getting rid of it, if possible, would be really expensive. The geometrical variation shown in parts is both size and form variation, while the variation in one assembly process comes from the variation in the contact between parts and assembly fixtures, variation in welding guns, etcetera (Wärmefjord, 2011).

PE Geometry (2015) defines geometry assurance as “All the activities and processes that are aiming to create a geometrically robust and well defined part/product that works both functionally and aesthetically in its geometrical surrounding”. According to Rosenqvist et al. (2014) geometry assurance refers to the engineering activities that secure that the geometry requirements are fulfilled in the product. The reason for having geometry assurance inside companies is that the parts have variation even if the same tools and processes are used in their production.

It is possible to predict the geometrical outcome of an assembled product through variation simulation. This can be done in the concept stage of the product development, having key characteristics and critical dimensions predicted. Regarding the variation simulation, there is a need to input digital models of the parts to be assembled in the form of meshes for non-rigid parts. They can be either modelled as rigid or non-rigid parts, the former being thick parts and the latter refer to thin sheet metal parts. The locating schemes and their tolerances are also required for performing the simulation. The purpose of a locating scheme or a positioning system is to fixate parts that will be later assembled or inspected in space. The good accuracy in the simulation is crucial in order to replace physical testing, showing benefits so as a shorter lead time and savings. Having accuracy in the simulation also includes reduced risks in misjudgements and therefore less scrap. Less scrap means supporting sustainability and improved work conditions (Wärmefjord, 2011).

According to Zhang & Wang (1994), the most important parameter in product and process design is the tolerance. It refers to the specification of a part to be accepted for a determined purpose. It is often specified by an Upper Specification Limit (USL) and a Lower Specification Limit (LSL). Additionally, the location schemes are also one of the main factors of the geometrical outcome of an assembly.

A variation analysis itself does not lead to low tolerances. Sufficient tolerance levels are the ones that fulfil the aesthetical and functional demands. These can be secured by having a robust design and a 3D variation analysis, where thousands of virtual assemblies are simulated in order to predict the geometry of the final product (PE Geometry Development AB, 2015).

RD&T (Robust Design and Tolerance) is software used as a support for the geometry assurance process, from the early design to the production phases. It acts as a statistical variation simulation tool that allows the product and assembly variations to be simulated, and thus, predict the outcome before physical tests are done (RD&T Technology, 2015).

2.2 Boron Steel

According to Bhat (2011), steel is the base material for current cars, making up to 62% of the weight. The use of Ultra High-Strength Steels (UHSS), which boron steel belongs to, is to meet the requirements of lightness, stringer safety regulations, emissions reduction, and performance. These are achieved by carefully controlling the chemical composition as well as the cooling and heating processes (Automotive Steel Definitions, 2015).

Boron steels are starting to be more common and used in wider applications. Their performance characteristics are achieved at a relatively low price through advanced manufacturing technologies (Frydman & Letkowska, 2012). It is added to both unalloyed or low alloyed steels to enhance its hardenability. This can happen even at very small proportions, of the degree of 0.001% boron content. But based on experience, the maximum hardness is reached when 0.0003 to 0.003% is added; adding more than that will start deteriorating it. This low quantity makes boron a more cost effective way of increasing hardness than other more expensive materials (Key to metal, 2007).

The hardness in steel is increased by boron only below the surface. In the microstructure level, boron has the effect of delaying the transformation of martensite to the bainite, ferrite and pearlite structures, which are softer. If boron were not present, these softer structures would be formed during the cooling process after austenitization, after annealing or hot working. The presence of carbon is also important for the hardenability of steel by using boron, since the effect of boron increases in inverse proportion to the amount of carbon present (Key to metal, 2007).

SAAB Automobile AB was the first automotive company who used boron steel for a component inside its SAAB 9000 (Berglund, 2008). After that, the number of boron steel components has been increasing. It is being used in parts such as the A-Pillar, B-Pillar, bumper, roof rail, rocker rail and tunnel (Karbasian & Tekkaya, 2010). The boron steel used on vehicles today has an extremely high strength, such as the one used in Volvo Cars, which has a yield point of about 1,350 to 1,400 MPa; that is around four times stronger than the average high strength steel (Key to metal, 2007).

The part that will be studied in this project is the A-Pillar for the all-new XC90 (See Figure 2) (Volvo Cars, 2013). This vehicle is built on the new Scalable Product Architecture (SPA), which contains over 40% of UHSS. This makes the safety cage a lot stiffer while keeping the extra mass (Volvo Cars, 2013). This part is made from Usibor 1500 steel, 22MnB5 boron steel with an Al-Si layer, which is a special kind of steel intended for hot stamping processes. According to ArcelorMittal (2014), the high strength of this boron steel makes it possible to have savings in weight from 30% to 50% in comparison to cold forming steel grades. The benefits are also stated as:

- It allows forming complex shapes due to its very good hot formability.
- Total absence of springback.
- Uniform mechanical properties through the part.
- Exceptional fatigue strength

Figure 2: XC90 Safety Cage (Volvo Cars, 2013)

Usibor 1500 is expected to have Yield Strength of 1100 MPa and an Ultimate Tensile Strength of 1500 MPa (therefore the 1500 in the name) after a hot stamping process. These values are higher than in other steels as seen in Figure 3 (Bhat, 2011). But it is in impact strength where the benefits of Usibor 1500 really come out. In a strength test shown by the steel supplier, a 1.5 mm thick beam is tested in a three point flexural test at 29 kph with a 10 kJ energy equivalent. The results are shown in Figure 4, which demonstrates the potential in weight reduction this material represents (ArcelorMittal, 2014).

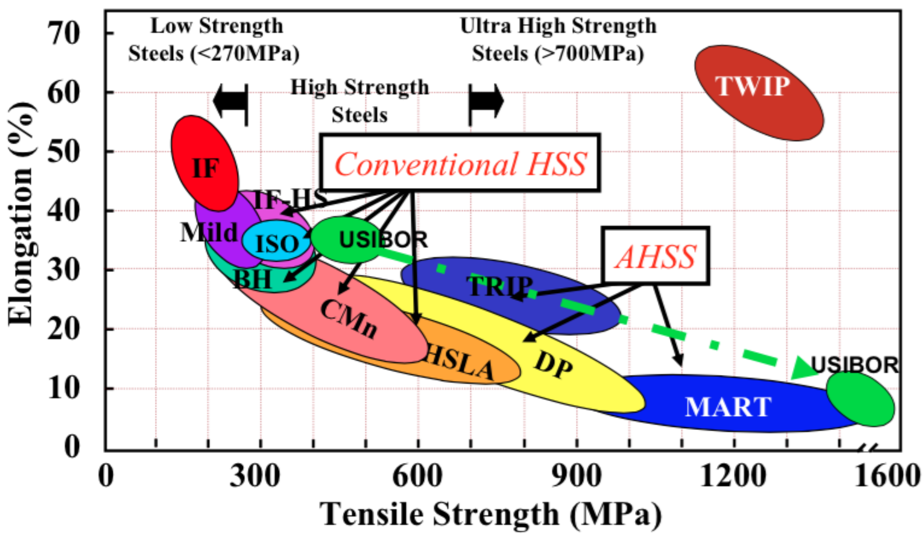

Figure 3: Steel type (Bhat, 2011)

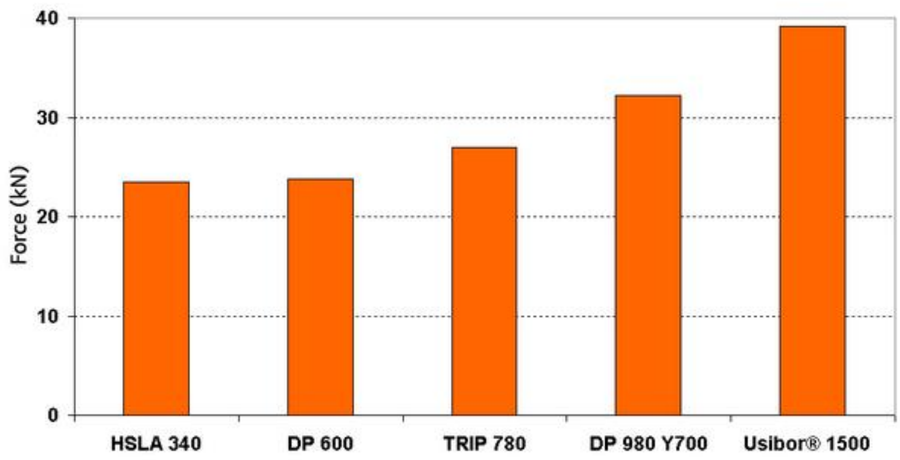

Figure 4: Beam results (ArcelorMittal, 2014)

2.3 Hot Stamping

2.3.1 Procedure

Due to the increasing use of UHSS in the automotive industry the need of manufacturing structural components in UHSS is apparent. UHSS has several disadvantages with respect to cold forming process. It has a very high hardness resulting in high impact on tools, reduced formability and a tendency to springback. Consequently, to improve the formability of materials such as UHSS, a new forming technology needed to be achieved. Hot stamping was developed first by a Swedish company, Plannja, in 1977 which used the forming process to produce saw blades and lawn mowers (Karbasian & Tekkaya, 2010). Today the same manufacturing method is used in the automotive industry for UHSS.

“Hot stamping is a non-isothermal forming process for sheet metals, where forming and quenching takes place in one combined process step” (Merklein & Lechler, 2006). There are several types of boron alloys that are able to produce fully martensitic microstructure after hot stamping: 22MnB5, 27MnCrB5, and 37MnB4 (Naderi, 2007). 22MnB5 steel grade is the most commonly used steel grade in hot stamping processes and automotive industry. Before the hot stamping process the base material, 22MnB5, has a ferritic-pearlitic microstructure with a ultimate tensile strength of about 600 MPa and yield strength 450 MPa. After it has passed through the hot forming process it has a martensitic microstructure with tensile strength of about 1400 - 1600 MPa (Merklein & Lechler, 2006). Table 1 shows the material properties of the 22MnB5 before and after hot stamping (Karbasian & Tekkaya, 2010). The hardness values were measured by Güler (2013).

Table 1: Material Properties of 22MnB5 before and after hot stamping

Steel	**Yield stress in MPa**		**Tensile strength in MPa**		**Hardness in HV1**	
	As delivered	Hot stamped	As delivered	Hot stamped	As delivered	Hot stamped
22MnB5	457	967	637	1478	191	483

There are two different methods of hot stamping, direct and indirect method. In the direct method the blanks are heated inside a continuous-feed furnace up to temperature between 900 and 950°C for 4 to 10 minutes. At that temperature the microstructure of the material transforms to austenite and has high formability, so that more complex shapes can be formed in a single stroke. Then it is transferred automatically to an internally cooled die within three seconds. Then the blanks are stamped and subsequently cooled down after the drawing depth is reached. During cooling process the formed part is quenched in the closed die that is internally cooled by water circulation at cooling rate of 50 to 100 °C/s. A diffusionless martensitic transformation will be induced, which is resulting in the high strength of the part and the part leaves the hot stamping line at 150 °C. The process of transferring, forming and quenching the part takes 15 to 25 seconds (Altan & Tekkaya, 2012). Figure 5 shows the transformation of the microstructure from austenitic at different cooling rates. As can be seen in the figure, to reach fully martensitic structure the cooling rate must be faster than 50 °C/s.

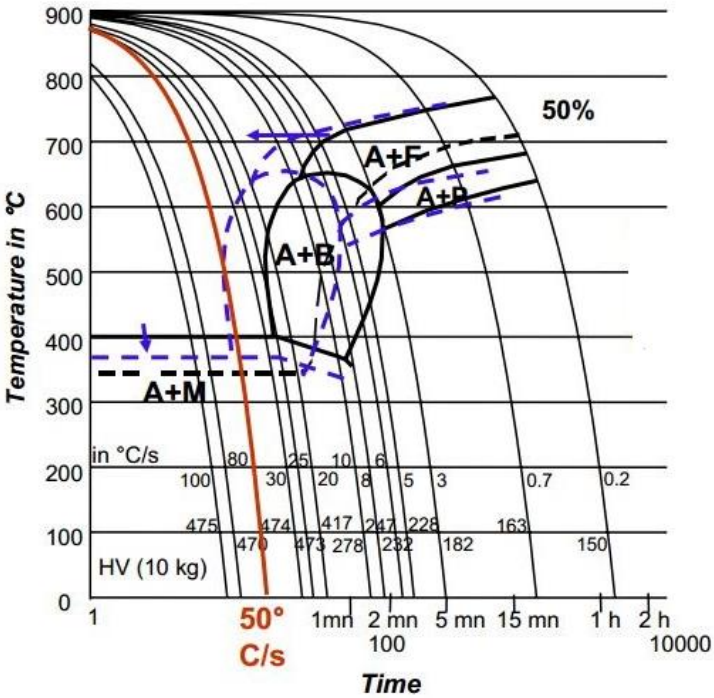

Figure 5: TTT diagram of USIBOR 1500P according to ArcelorMittal (Merklein & Lechler, 2006)

In contrast, during the indirect process the blank is first cold drawn, unheated, to approximately 90% of final shape. Then, the preformed parts are heated to austenization in a furnace and quenched in the die. The reason behind this method is to reduce the wear in the die because the relative movement between die and blank during hot forming process results in heavy wear on the surface of die. Figure 6 and 7 illustrate the two methods (Merklein & Lechler, 2008).

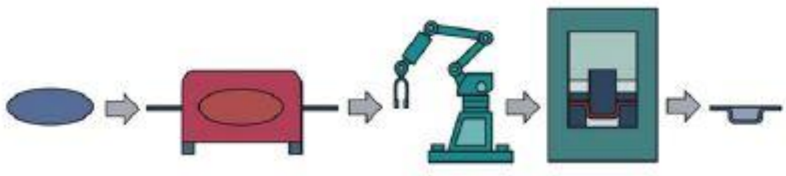

Figure 6: Direct hot stamping process (Merklein & Lechler, 2008)

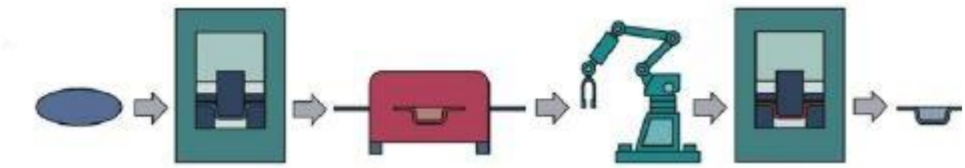

Figure 7: Indirect hot stamping process (Merklein & Lechler, 2008)

2.3.2 Residual stresses

Almost all manufacturing processes develop residual stresses (Verlinden *et al.,* 2007). Residual stresses are the locked-in stresses in a body that is free of external forces or thermal gradients. Residual stresses increase due to thermal and mechanical treatment (Pfeifer, 2015). In Figure 8, the atomistic origin of residual stress is described in details. The initial lattice structure of the material is imposed by external stresses which results in structural changes of the lattice. When the stresses are removed, the changes in the lattice become permanent, constraining for example elastic recovery. These are the residual stresses (Verlinden *et al.,* 2007).

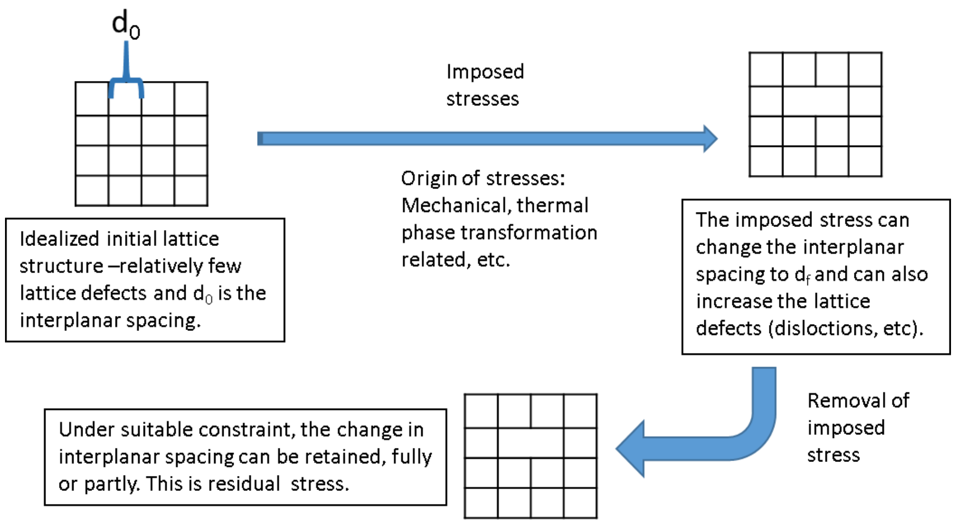

Figure 8: An undeformed material with an interplanar spacing d_0 is subjected to impose stresses (mechanical, thermal, phase transformation etc.). This could cause changes in the interplanar spacing and lattice defects (dislocation, stacking fault, etc.). After releasing the imposed stress the interplanar spacing (elastic strain) is retained, fully or partly. (Verlinden et al., 2007)

Hot stamping is a thermo-mechanical forming process (TMP) with intended phase transformation where relatively simple, basic materials are converted into high quality components by heating and shaping. The material is treated both mechanically and thermally which generates mixture of residual stresses and the mechanical and thermal properties of the material varies with temperature and deformation during the TMP.

As with most metal-forming operations hot stamping has two consequences. "On a 'macroscopic scale' the desired shape change is obtained and on a 'micro scale' the microstructure of the material is changed" (Karbasian & Tekkaya, 2010). Similar phenomena can be explained with residual stresses. The microscopic stresses occurring in a body can vary inside a grain due to the presence of inclusions, dislocations, stacking faults, etc. It can also vary between the grains or crystallites, since each grain orientation possesses specific elastic and plastic properties. Finally, these two micro-stresses combine and form macro-stresses (Verlinden *et al.,* 2007)..

When the part is heated, like done in hot stamping, residual stresses arise due to volume differences between the new, austenite, and initial metallurgical phases, ferritic-pearlitic. The volume difference results in material expansion or contraction because during cooling the outer portions of the metal cools first and undergo the phase transformation. During quenching the transformation from austenite into martensite causes increase in volume which influences the stress distribution in the part (Figure 9) (Pfeifer, 2015).

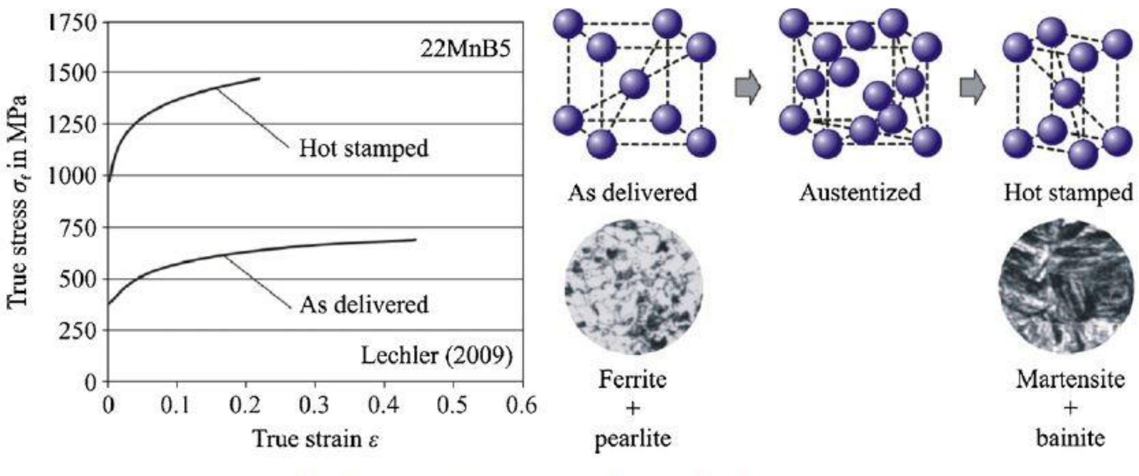

Figure 9: Flow curve and microstructure of 22MnB5 during hot stamping (Karbasian & Tekkaya, 2010)

If the phase transformation occurs without applied stresses the material response would be purely volumetric. In the case of hot stamping the transformation occurs under an external stress, inside a die, and causes irreversible deformation. This is called transformation-induced plasticity (Karbasian & Tekkaya, 2010). Residual stresses arise when non-uniform distribution of plastic strain, e.g. permanent deformation, occurs in a deformed part. This is explained in figure 10. The surface of a part has been plastically deformed in tension by bending. After the external force has been released the regions that have been plastically deformed prevent the adjacent regions from undergoing complete elastic recovery (Pfeifer, 2015). When modelling the thermoplastic behaviour during hot stamping, the strain increment can be described by the sum of elastic, plastic thermal and isotropic transformation, and transformation-induced plasticity strains (Karbasian & Tekkaya, 2010).

Figure 10: Residual stresses during bending (Pfeifer, 2015)

If the residual stresses in metal are large enough they can cause distortion or cracking. "Distortion can occur when the residual stresses (or portion of it) in a body is eliminated" (Sinha & Division, 1991). So, controlling the magnitude of the stresses is often very important. That can be achieved with heat treatment processes, right material selection and controlling the cooling rate. Heat treatment such as stress relief annealing is common where the part is heated to recommended temperature, held there for long enough to attain uniform temperature and finally cooled to room temperature.

Not all residual stresses are bad, depending on whether the stress is tensile or compressive. In some manufacturing processes, such as shot peening and light cold rolling, they induce a compressive residual stress at the surface of a component for the purpose of improving resistance to fatigue and stress corrosion cracking (Pfeifer, 2015). On the other hand, residual tensile stresses at the surface are usually harmful; they can cause unpredicted stress-corrosion, cracking, or fatigue failure, which tend to reduce the fatigue life and strength of a part. Residual tensile stresses in the interior of a part may also be detrimental (Sinha & Division, 1991).

2.4 Laser Process

The laser was invented in 1960 without having the application possibilities discovered. In the end of 60's companies started to use a manufacture laser commercially and in 1970 the automotive industry started to realize their potential for material processing. Today it's a different story and the application area is wide and diverse. Laser is known now for precision, quality and speed and it thus provides opportunities for innovation in material processing (Icon, 2005).

Industrial laser is a flexible machine tool that produces a beam of light with unique properties. The light can be controlled accurately providing an intense source of energy that is ideal for penetrating materials. The mode of beam-material interaction can be either thermal or athermal. During the thermal process a certain portion of the incident light energy is absorbed by the material (photon absorption) and high temperature is developed in the vicinity of beam spot, resulting in heating, burning, melting, evaporation, local yielding or material softening. "The beam can be manipulated with optical components to perform a variety of operations simultaneously, or switched between locations for sequential processing" (Icon, 2005).

The mechanism of thermal interaction, heating, melting or vaporization, between the laser beam and the material is illustrated in Figure 11. Considering surface heating a stationary laser beam of circular cross-section heats the surface of a large block of material. When the beam hits the surface the heat flow becomes steady state, meaning that the energy absorbed by the surface is balanced by what is conducted into the block. The temperature field around the heat source becomes constant. To principal process variables of laser processing are the beam power, q, the beam radius, r_B, and material properties. These variables form the power density, E:

$$E = \frac{q}{(\pi \times {r_0}^2)}$$

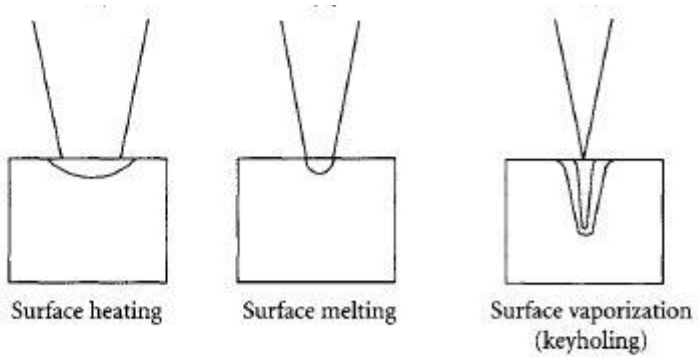

Figure 11: Interaction mechanism between a laser beam and a large block of material (Icon, 2005)

A lot of different types of industrial lasers are existing depending on their active medium (gas, liquid or solid), wavelength, power, energy and mode of operation (continuous or pulsed). Steen (2003) discusses five main types of industrial lasers; CO2 laser, CO laser, solid state laser, diode laser and excimer laser. Solid state lasers have a solid active medium rather than gas or liquid. "In comparison with gas lasers, solid state lasers require no mechanical devices for media circulation, complex heat exchangers, or vacuum and gas-supply systems" (Icon, 2005). On the other hand, the thermal conductivity of the material host determines the amount of heat generated.

2.5 Martensite tempering

2.5.1 Procedure

Martensite is a very hard phase in steel and due to that and its high yield- and tensile strength it can be very useful in some areas. Martensite is normally too brittle for many applications so the mechanical properties need to be modified by heat treatment. The ductility and toughness is enhanced at the expense of material strength and the internal stresses that are introduced during quenching, are relieved. This process is called tempering, often referred to as martempering (Bhadeshia, 2015).

The reason why martensite has so high hardness is because of strong supersaturated carbon in the iron lattice of the martensite structure. The lattice has a high density of distortion, e.g. defects, dislocations, and high- and low-angle boundaries, meaning that a lot of residual stresses exist in the structure. The high lattice distortion induces high hardness and strength to the steel.

The process of tempering the martensite describes how the microstructure and mechanical properties change as the sample is held isothermally at a temperature close to or below transformation temperatures (A_{C1} line) irrespective of the manufacturing process. It is carried out at the temperature range 150-700 °C, though it depends on alloying constituents and time (Figure 12). Internal stresses, however, may be relieved at a temperature as low as 200 °C. During the tempering process, the martensite forces the carbide to precipitate and the formation of tempered martensite happens according to the reaction (Callister, 2007).

Martensite (BCT, single phase) → Tempered martensite (α + Fe_3C phase)

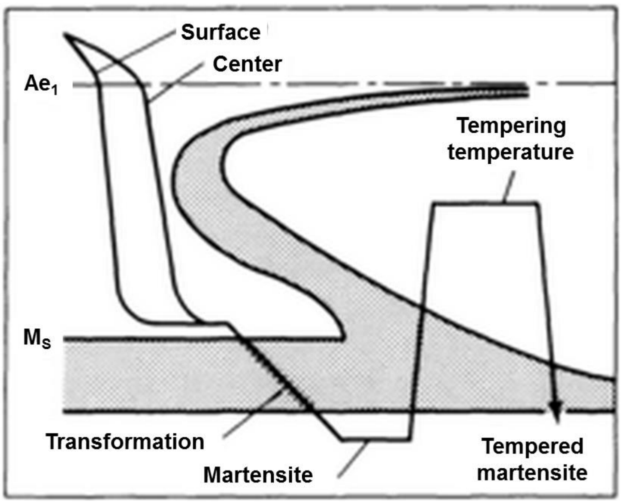

Figure 12: The temperature transformation diagram of quenching and martempering (Webster & Laird, 1991)

The tempered martensite is not as hard and strong as martensite, but it has substantially enhanced ductility and toughness. The microstructure consists of a very fine and small cementite particles embedded with ferrite matrix. What defines the new hardness and strength of the tempered martensite is the ferrite-cementite phase boundary area per unit volume of the fine cementite particles. The hard cementite phase reinforces the ferrite along the boundaries, making it strong and hard, but the continuous ferrite phase makes the material also very ductile and relatively tough, which accounts for the improvement of these two properties for tempered martensite. The sizes of the cementite particles (Figure 13) plays essential role in determine the material behaviour of tempered martensite. Increasing the particle size decreases the ferrite-cementite boundary area, resulting in softer and weaker but yet more ductile and tough material and vice versa (Callister, 2007).

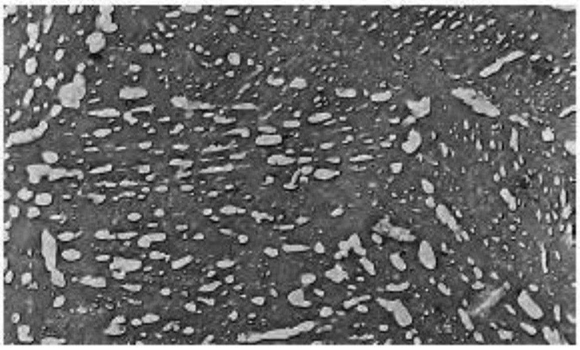

Figure 13: Electron micrograph of tempered martensite. Tempering was carried out at 594 °C. The small particles are the cementine phase; the matrix phase is α-ferrite. (Callister, 2007)

The heat treatment variables, temperature and time, determine the size of the cementite particles and the final material properties. Increasing tempering temperature accelerates the carbon diffusion in the martensite-tempered transformation, the rate of cementite particle growth and rate of softening (Callister, 2007). Table 2 shows the four distinct and overlapping stages that take place during reheating of as-quenched martensite material (Key to metal, 2015):

Table 2: Stages of tempering martensite

Stages of tempering martensite	
Temperature range	**Reaction**
Up to 250 °C	Precipitation of transition carbides (α-iron carbide); partial loss of tetragonality in martensite.
200-300 °C	Decompositions of retained austenite
250-350 °C	Replacement of α-iron carbide by cementine; martensite loses tetragonality
Above 350 °C	Growth and spheroidization of cementite and other carbides; recrystallization of ferrite

The tempering process can be divided into two categories; isothermal, like has been described, and non-isothermal tempering. Isothermal process includes the conventional heat process, slow heating, long holding time at peak temperature and slow cooling. Non-isothermal tempering occurs with manufacturing process such as welding and joining involving rapid heating, negligible holding time and rapid cooling. There is little work found about the temperature behaviour of non-isothermal tempering process.

Because of negligible holding time the non-isothermal process is strongly affected by the heating rate. This is very vital when it comes to choosing a suitable manufacturing tool for the tempering process. Take for example lasers, diode laser during welding produces much more severe softening because of its slower heating rate compared to Nd:YAG lasers (Baltazar Hernandez et al., 2011). According to Furuhara et al. (2004), increasing the heating rate during non-isothermal tempering of fully martensite steel, would result in refinement of cementine particles which is crucial for controlling the balance between the strength-ductility of the material.

2.5.2 Defects and distortion in heat-treated parts

Distortion can be defined as all the irreversible dimensional changes produced during heat-treatment operations. The term irreversible change refers to changes in size and shape that are caused by stresses above the elastic limit or metallurgic structure change, such as phase transformation.

Size distortion occurs when the nominal part changes in volume. Shape distortion is a change in a geometrical form of the part like curvature, bending, twisting, and/or non-symmetrical dimensional change without any volume difference. Often combinations of both cases take place during a heat-treatment process.

During tempering of martensite a correlation can be found between the tempering temperature and volume change. Tempering reduces the volume constituent of martensite in material but the decrease is less than the total volume increase of the part as a result of martensite transformation. During the first and third stage of the tempering process (Table 2) precipitation of carbon occurs and replacement of cementite particles embedded with ferrite takes place. On the other hand, during the second stage an increase in volume takes place due to the decomposition of the retained austenite. As the tempering temperature is increased further toward the A_{C1} line the more volume reduction arise (Figure 12). Finally, when the part is cooled down from the tempering temperature an additional increase in volume will occur because of transformation of retained austenite into martensite.

Shape distortion is a change in a geometrical form of the part like curvature, bending, twisting, and/or non-symmetrical dimensional change without any volume difference. It is usually not as predictable as size distortion and often of greater magnitude. The factors for shape distortion are several and will be listed here (Sinha & Division, 1991):

- Non-uniform heating and cooling.
- Residual stresses present in the part before the heating process.
- Applied stress causing plastic deformation. Sagging and creep can happen during the heat treatment if the components are not properly supported. So, complex shaped parts should be supported in critical positions during the process.
- Non-uniform quenching. Uneven hardening, with the formation of soft spots increases the distortion.

- “Tight (that is, thin and highly adherent) scale and decarburization, at least in certain areas” (Sinha & Division, 1991).
- Long parts with small cross sections where L is the length of the part, and d is its diameter or thickness:
  - L >= 5d for water quenching.
  - L >= 8d for oil quenching.
  - L >= 10d for austempering.
- Thin parts with larger areas where A is the area of the part, and t is its thickness:
  - A >= 50t
- Unevenness in the part section.

2.6 Boron Steel Laser Welding

Kim, Kang and Park (2011), studied the changes in boron steel after welding. The study is done on boron alloyed steel, after being hot formed and successively quenched. When welding hot forming steel with Al-Si coating, the coating is melted into the weld zone creating a zone with Fe-Al intermetallic phase. The brittleness of this phase weakens the strength of the joint.

The input of heat during the welding process transforms the martensite structure in the base metal. Outside the Heat Affected Zone (HAZ), the maximum achieved temperature is lower than AC3 (Figure 14A), which resulted in tempered martensite with softer properties. The white band area reached a temperature between AC3 and AC1 that resulted in bainite (Figure 14B). The inner HAZ was heated to a temperature in between AC1 and melting temperature, which came to be a mix of martensite and bainite (Figure 14C). In the fusion zone, the melting and successive quenching created a martensitic microstructure (Figure 14D). In Figure 14E, the microstructure from the base material is shown.

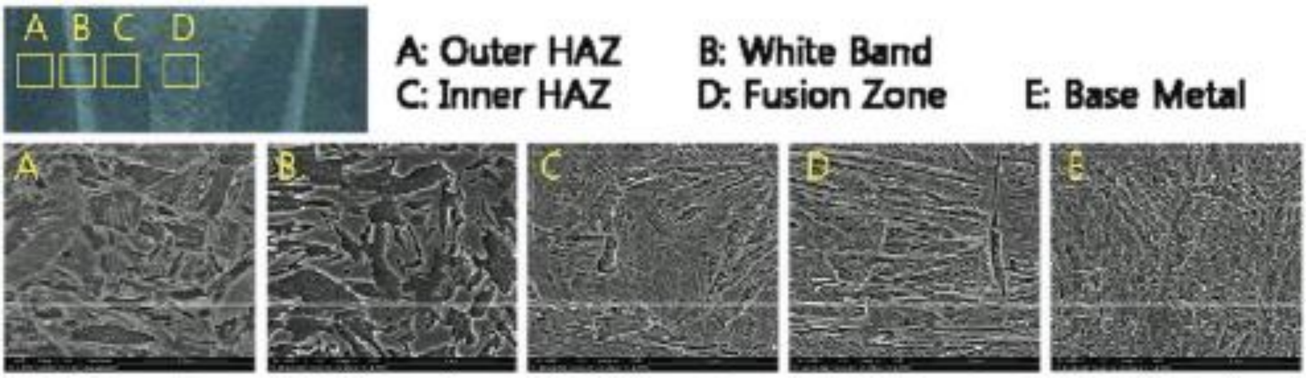

Figure 14. Material Changes in Boron Steel when Welded. (Kim, Kang, & Park, 2011)

When welding, the goal is to have the minimal impact on the microstructure, and the mechanical and chemical properties. An UHSS like boron steel has very valuable properties that should be kept. A way to maintain these properties and increase the quality of spot weld is by point tempering the part prior to the welding process. “Bringing the material up to a specified temperature before welding can help reduce the residual stresses in the material and prevent it from cooling too quickly, which causes changes to the material's microstructure that lead to cracking, distortion, and softening" (Packard, 2012).

2.7 Welding Sequences

The Travelling Salesman Problem (TSP) is a mathematical problem where a salesman is supposed to visit a set of cities once and then going back to where it started. This problem is relatively easy when the set of connecting points is small, but its complexity increases as the number of cities increases. The method used to solve the TSP is through an algorithm that will provide an efficient solution for a specific scenario, but it is not expected to find an algorithm that can efficiently solve every single TSP. But there are some algorithms that provide a good enough solution with reasonable computation time (Klarreich , 2013). Some methods for optimizing sequences are:

1) Simulated Annealing Temp: Not to be confused with the metals heat treatment, it is an algorithm that is also based on finding local minima by wandering from neighbour to neighbour to find a better result. The difference from other methods is that this wandering is done randomly, so it does not get caught at local minimums (Johnson & McGeoch, 1995).

2) Genetic Algorithms: Is an adaptive heuristic method that mimics the evolutionary ideas of natural selection and evolution. It uses the intelligent search of randomized solutions to find a solution for optimization problems. Via selection, crossover, and mutation it will converge over successive generations towards the global optimum (Drossopolu, 1996).

According to Wärmefjord *et al.* (2010), it is common to use genetic algorithms related methods to establish welding sequences. However, they have the drawback of needing several FEM simulations and therefore lots of time, and also the disadvantage of not providing clues about why some sequence is better than the other. When welding, the geometry points should be welded first since they lock the part into position, so that it can be released from its fixtures. Still, different welding sequences provide different results due to the fact that forces are being applied differently resulting in different displacements in the final assembly. There are four strategies suggested by the authors:

- Strategy 1: General simple guidelines.
- Strategy 2: Minimization variation in each step.
- Strategy 3: Sensitivity.
- Strategy 4: Relative sensitivity.

Strategy 1 can be related to the work described here, since it provides general guidelines to establish a welding sequence such as always starting from the middle towards the outer edges, or starting from the outer edges to the middle. If distortion occurs at one point and not in the others, the suggested guidelines are to start in the distorted point always or to always finish in the distorted point. The other three strategies are related to welding points and the deformation caused by the fixing of the part, so they are not covered in this work.

2.8 Summary of Literature Review

The automotive industry is being pushed to innovate because of regulations and as a response to the high demands of safer vehicles, better quality and lower fuel consumption. Manufacturers are changing to newer materials that have higher strength and reduced weight. Boron steel is a part of family of steels known as Ultra High Strength Steels, which contributes to the reduction of the mass in the vehicles and increases its safety for passengers. The reason to use boron is its cost effectiveness compared to other alloy substances when increasing steel hardness. This increased hardness calls for new processes that represent new challenges to solve, in this case, joining a very hard steel with other materials. This cannot be made through welding, since some materials are composites, so mechanical joining seems to be the solution to this.

The part to be studied in this work is an A-Pillar of Volvo Cars XC90 Model, after it has been formed with hot-stamping. This process consists of heating the part, and then stamping it and cooling it down really fast simultaneously. This process generates residual stresses in the part, both thermal and mechanical. The main causes for those stresses are:

- Material expansion due volume difference between austenite and martensite phase during phase transformation in the metal.
- Non-uniform distribution of plastic deformation of the part.

After the hot stamping process, the part has a martensite structure, which is a very hard phase with high yield. The high hardness of the part and the possible consequences of internal stresses require further processes, such as local softening for the former or stress releasing for the latter. In this work, laser tempering is used to locally soften the material, to increase its ductility and toughness, so that is easier to later self-pierce rivet the material. The part is locally tempered, non-isothermally, by heating it within a range of 150-700 C, followed by fast cooling down to room temperature. A possible consequence of heat treatments, i.e., applying heat to the part to modify its material characteristics, is deformation: shape and size distortions. This happens because residual stresses are present in the part, non-uniform heating and cooling, volume changes, etc.

When the geometry of the part gets deformed it can cause difficulties in the consequent assembly process, since variation may cause that the functional or aesthetics requirements are not met. Geometry assurance is related to all the activities that take place in order to keep the geometrical variation under control. One of the tools that geometry assurance uses is variation simulation. The software RD&T is a tool that predicts the variation of the part after heat is applied, thus, saving time and capital in physical parts.

There is not enough information about tempering of boron steel, but there is a relation with locally applied heat in the form of boron steel welding. The material structure and characteristics change because of the intense temperature, even in areas outside the fusion zone. There is evidence that show that there is a relation between the welding sequence and the geometry response. Several optimization techniques exist for establishing sequences, a lot of them where developed focusing on solving a well-known problem titled Travel Salesman Problem. The selection of an algorithm to solve TSP depends on the amount of testing. But there are general guidelines suggested that can be applied to the project's sequence selection. The distortion that occurs in the cases of welding is described as a consequence of fixing the parts together and not as a result of heat effects. Since the distortion during tempering occurs for different reasons, the methods developed for welding cannot be directly used in this case, but the general algorithms and guidelines act as useful tools.

3. Defining Laser Parameters

3.1 Previous tests

This section presents previous studies and tests done by Swerea IVF and VCC. These tests are important to the thesis study, both to understand what initiates the need for finding a method for minimizing the distortion and to investigate the required tempering hardness of boron steel with the right set of laser parameters.

3.1.1 Self Pierce Riveting

Swerea IVF and VCC have been developing mechanical methods for joining carbon fiber and boron steel (Usibor 1500) and one of their solutions is using self-pierce rivet. Self-pierce riveting (SPR) is a mechanical fastening process for point joining of sheet metals. It generates dynamic strong riveted joints, it has double strength against clinching, it has high-energy absorption (stress-strain curve) compared to welding (Figure 15) and it brings the possibility to join two or more materials together. Figure 16 shows general rivet joining and its process parameters. “The rivet pierces the top sheet and the die shape causes the rivet to flare within the lower sheet to form a mechanical interlock” (TWI, 2015)

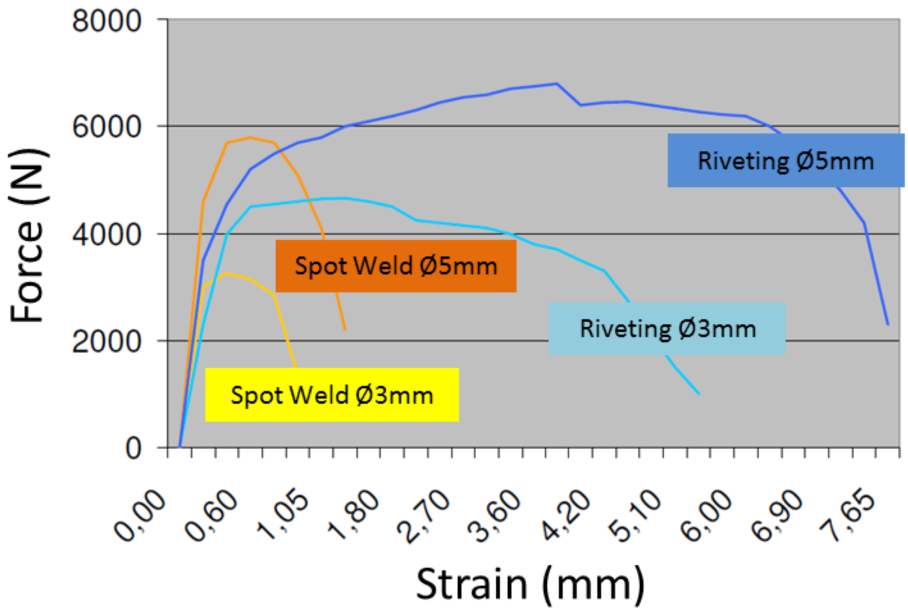

Figure 15: Stress-strain curve of welding and SPR (Hansson, 2015)

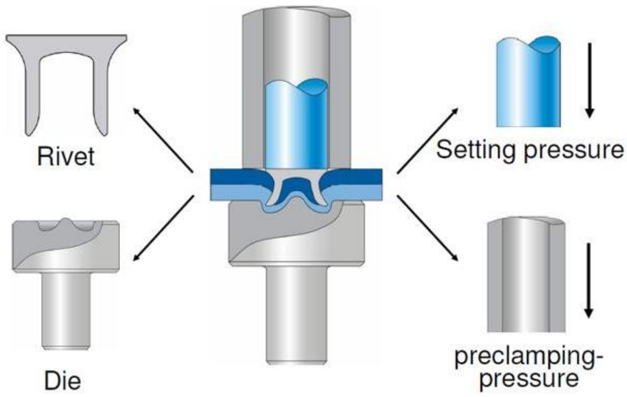

Figure 16: Parameters of a riveting joint (Hansson, 2015)

Since the intention is to join a composite material with a metal, by using a metallic rivet, it is necessary that the bottom sheet is ductile so that the rivet forms the mechanical interlock. Since composites are not ductile, it was decided to use an aluminium coin as the third and bottom material. When doing SPR, the rivet needs to be harder than the top sheet, and the bottom sheet needs to be softer than the top one. Therefore, it was necessary to soften the top material, which is boron steel, by tempering it before the SPR process.

Several combinations of SPR parameters have been tested, e.g., rivet hardness, different rivet shank geometry, or coin thickness. As mentioned in Chapter 2.3, the part leaves the hot stamping process with a hardness of approximately 500 HV and after the points are tempered, the hardness level drops. From what Swerea IVF and VCC have been testing and investigating, the necessary hardness to conduct SPR in boron steel with martensite phase is at least 300 HV. With this as a target hardness value there is a need to establish the laser parameters to reach it and its resulting temperature. Table 3 includes the rivet alternatives according to its hardness (Hansson, 2015).

Table 3: Alternative hardness (Hansson, 2015)

Alternative Hardness
H0 (280 ± 30HV 10)
H2 (410 ± 30HV 10)
H4 (480 ± 30HV 10)
H5(510 ± 30HV 10)
H6 (555 ± 30HV 10)

3.1.2 Laser tempering with random sequence on A-pillar part

As a part of the PLUGG project, Swerea IVF and VCC, tested the hardness reaction of boron steel when it is heated with a laser, during spring/summer 2014. Series of boron steel coupons of 125 x 38 mm were locally heated with a laser for 1.5 seconds and 2.3 kW of power. The laser model used for this was Trumph type TruDisk 4002 with a Scansonic ALO3 head.

The tests prove the fact that the hardness of the material decreases when the laser-power is applied. It also shows that the heat-affected zone is larger than the laser beam area (red circle), as seen in Figure 17. The hardness in the centre of the laser dropped to approximately 280 HV while the base material has 500 HV.

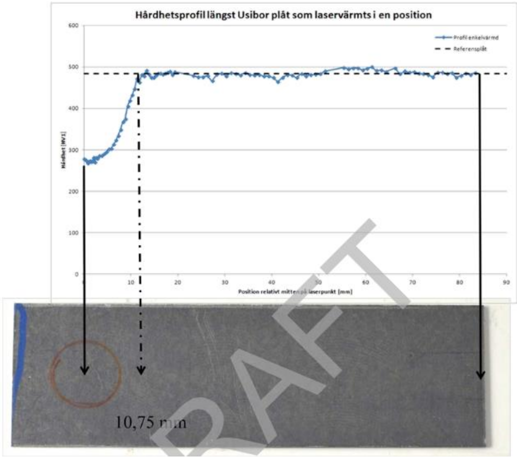

Figure 17. Hardness Test Coupon (Wandebäck & Albinsson, 2014).

To investigate this matter further and how it responds to heat, same test was conducted on the A-pillar part. A randomly selected sequence was chosen, consisting of points scattered through the flanges of the A-Pillar every 40 mm. The start and finishing points are shown in Figure 18.

Figure 18. Testing Sequence Start and Finish.

The response in the part's geometry to local heating using the aforementioned sequence was distortion and can be seen in Figure 19. Five pieces were tested, 3D scanned before and after, and all of them showed the same distortion. The results from the scanner were analysed by using GOM Inspect software. The biggest deformation occurs in the centre of the part and on the inner flange (Wandebäck & Albinsson, 2014).

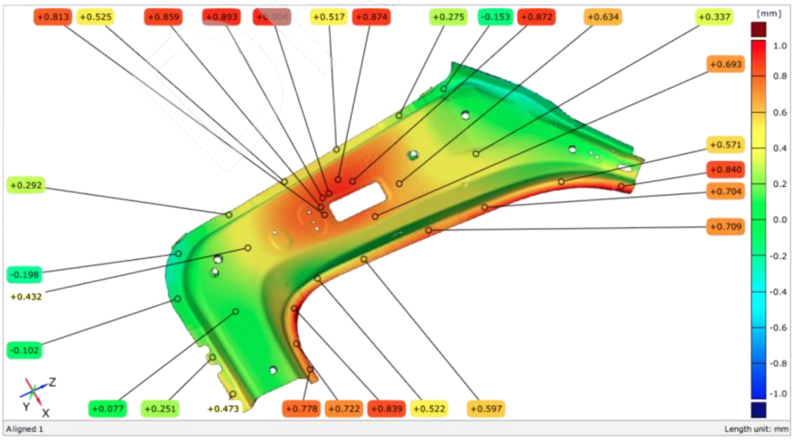

Figure 19. Distortion in Test Part (Wandebäck & Albinsson, 2014).

3.2 Laser & Hardness Tests

Laser tempering and hardness tests were done in a corporation with Swerea IVF and VCC where the aim was to investigate how different laser-powers at a fixed time, 0.5 sec, affect the material hardness and how much temperature it generates. The earlier SPR tests (section 3.1.1) prove that the sufficient hardness for making good SPR is around 300 HV and consequently it will be the target hardness value for the following tests. The tests were conducted using the same laser as previous tests (Section 3.1.2) on Usibor 1500 coupons, with a thickness of 1.0 mm, which have already been quenched to martensite structure. Three points were tempered with the laser beam diameter of 1.38 mm and different laser power settings (0.75, 1.25, 1.50, 1.75, and 2.00 kW) for each coupon, followed by air-cooling to room temperature.

Pyrometers were placed on both sides of the coupon to measure the temperature during and after the tempering process. The intention was to understand the heat distribution in the part, measure the maximum temperature reached, and to calculate the cooling rate down to 150 °C.

The temperature curve for each test is plotted and illustrated in Appendix I. In order to understand the temperature that is reached with each laser power setting, and how the heat is distributed, a curve for maximum temperature at each power setting is plotted for all the points (Figure 20). By comparing the curves, it is possible to notice a small difference between each point at each power setting. On the other hand, even if there is a difference between maximum temperature on the front and backside, the curves are practically parallel. This shows that the heat is not uniformly distributed throughout the part. Increasing the laser time is expected to generate a more uniform distribution of the heat at the expense of increasing the size of the heat affected zone, as well as the process lead time. The trade-off consists of a balance between the maximum acceptable heat affected zone and temperature difference between the two sides.

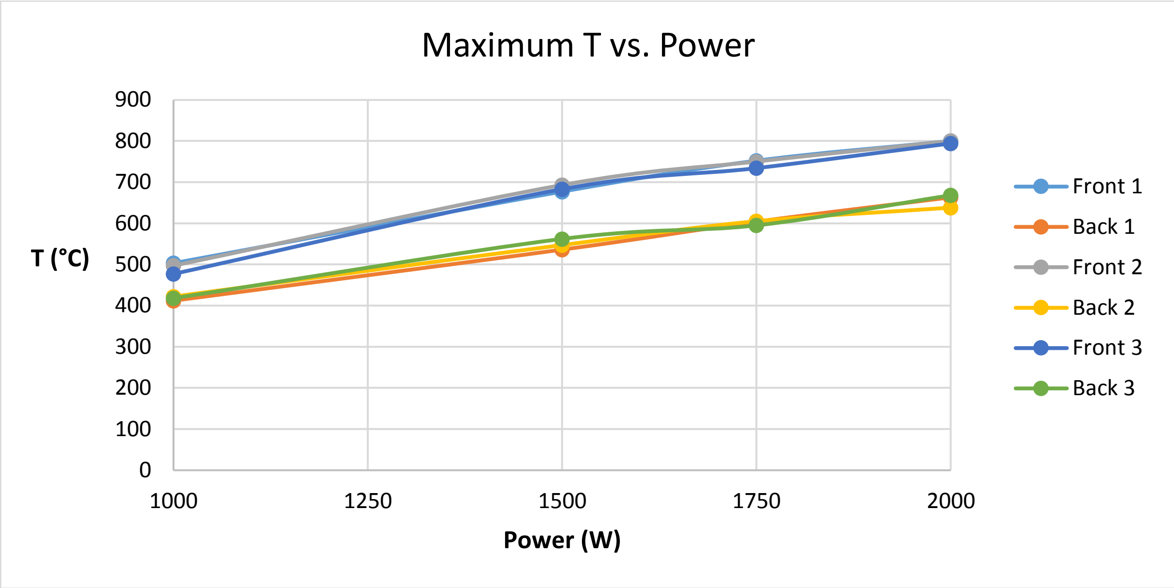

Figure 20: Maximum temperature for each tempered point vs. power

Cooling time, closely related to the method employed, is an important factor that defines the qualities of the material after the tempering process. In this case, the coupons were air-cooled rapidly at room temperature. The cooling time is considered to be fast, within a range of 50-66 °C/s for the front face and 39-54 °C/s for the backside; it is worth to mention that the higher laser power used, the slower the cooling rate is. There is also a difference between the cooling time of the front and the backside, the latter having a 3.7% slower cooling rate. The reason for such rapid cooling is the relative small thickness of the coupons. The thinner the heated plates are the less energy they can store, which results in rapid cooling.

Test results show how much heat is generated at different laser-power and how it distributes through the part. It also confirms that temperature descends by cooling the part with still air at room temperature. Even though, the tempering time was not sufficient to generate uniform heat through the part, the difference is less than 5% and will likely not cause a problem for the next manufacturing step, self-pierce riveting. Regarding the cooling time, with rapid cooling it is important to produce mild agitation cooling, such as still air, to avoid large temperature differences, e.g., uniform cooling, and thereby minimize the distortion.

Each coupon with its respective three laser tempered spots were later analysed for their hardness at Swerea IVF facilities. The intention is to find out the relationship between the laser power employed and the consequential drop in hardness and size of the heat affected zone. A continuous set of points was measured for hardness in a cross-section of the coupons, with a denser grid of measuring points around where the laser was applied as seen on Figure 21, while the results are shown in Table 4.

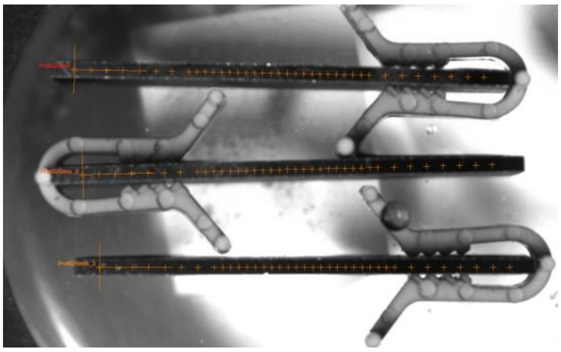

Figure 21: Hardness Test Points Position at 1.0 kW.

Table 4. Laser Power vs. Hardness.

Laser Power	Front Max Temperature	Back Max Temperature	Original Hardness	After Laser Minimum Hardness	Heat Affected Zone Width
kW	**°C**	**°C**	**HV1**	**HV1**	**mm**
1.00	492	417	514	408	14.5
1.25	N/A	N/A	507	371	16
1.50	684	588	506	320	18.5
1.75	745	601	510	304	20.5
2.00	798	656	500	282	20.5

The values for the original material hardness are the points located at the edges of the coupons, where neither the laser nor the transferred heat affects the material properties. The minimum hardness obtained was taken from the average of the lowest value for each tested point, while the heat affected zone width was measured when the hardness values start to change compared to the original material hardness (Figure 22 and Appendix 3).

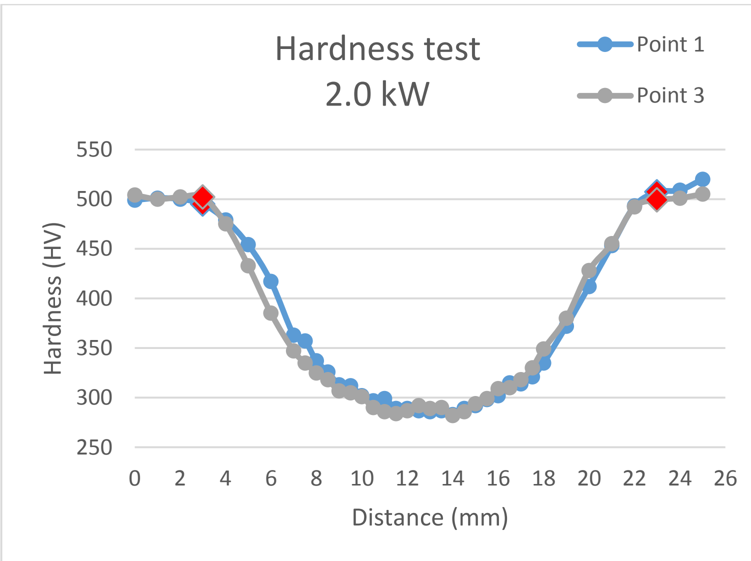

Figure 22: Hardness value for each tested points on cross-section of the coupon.

The hardness was measured with respect to the surface, top and bottom, and no significant change in hardness values was visible, as seen in Figure 23 despite the meaningful difference in temperature between each face as stated in Figure 20. The temperature difference could be even higher between the two faces, suggesting big differences in material hardness depending on the thickness. On the other hand, the uniform temperature through the thickness of the material, and therefore its consequent homogeneous change in hardness, is not required for the SPR process as stated by Hansson (2015).

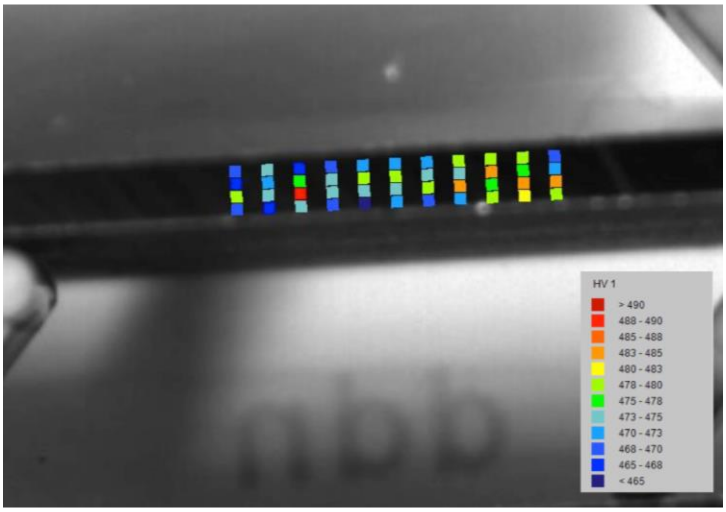

Figure 23: Hardness Levels Relative to the Surface

Another visible effect the laser had on the coupons was distortion. It is possible to appreciate that the coupon bent when 2 kW power were used, as opposed to Figure 21 where no visible deformation occurred with 1 kW. To get a numerical prove of the distortion in the coupons, they should have been scanned before and after the tempering process. Nevertheless, the main focus with the tests was obtaining the required laser settings and reflecting temperature, the scanning of the coupons was not considered relevant.

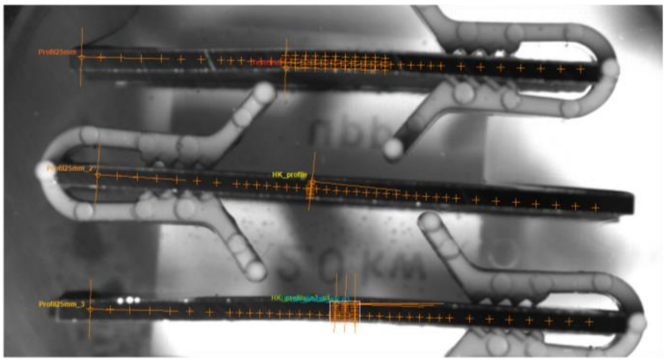

Figure 24: Distortion at 2 kW

3.3 Laser Parameters Results

To retrieve the target hardness value of 300 HV after tempering, established by Swerea IVF and VCC, the necessary temperature and laser parameters are:

- Laser power: 1.75 kW
- Laser time: 0.5 sec
- Laser beam diameter: 1.38 mm
- Resulting avg. temperature: 673 °C
- Resulting maximum temperature: 745 °C
- Resulting HAZ: 20.4
- Resulting hardness: 304 HV

4. Sequences

In this chapter the goal is to find a relation between tempered sequence and distortion on the A-pillar. The first goal is to prove if there actually exists a relation by simulating the tempering process and then verify the results with physical tests. The following objective is then to advocate for the sequence that gives the minimum distortion among them.

The simulation tool used is the newly developed RD&T Heat Analysis module. Observations about the functionality and the interface of the software are done in chapter 5.

The amount and location of heated points in the A-pillar is considered irrelevant in any of the tests since the goal is only to compare different sequences. Although, it is crucial to analyse the same set of points in all the sequences when performing simulations or physical tests.

4.1 Simulation of the tempering process

The heat analysis of the tempering process was simulated by using RD&T. The purpose of the simulation is to see the relation between sequence and deformation to later verify them with the results of a physical test.

In Figure 25, the five sequences that were simulated (A, B, C, D and E) can be seen. The main objective was to choose sequences that are very different among them, in order to clearly distinguish the impact they have on the parts. Sequence A follows the idea of having the tempering points from the outside to the inside of the part. The sequence B follows the opposite, from the inside to the outside of the part. Sequence C works under the idea of minimizing the distance between tempering points, therefore it follows a continuous line on the flanges of the part. The D and the E sequences try to maximize the distance between the points. Details can be found in Appendix IX.

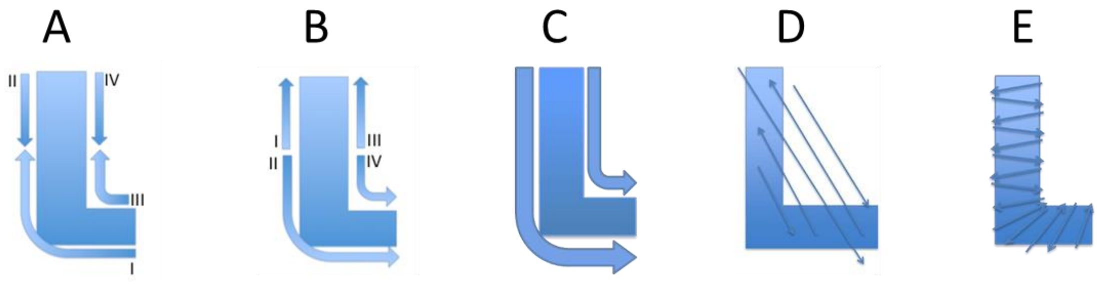

Figure 25: Simulated sequences using RD&T

4.1.1 The Heat Analysis Model

Next will be a brief description of the mathematical model behind the simulation in order to understand how the deformation calculations occur. Subsequently, the FE model and the material properties are described, and finally results are revealed.

The heat calculation is a standard finite element heat transfer model. It is non-linear finite element analysis taking into account the blackbody radiation and heat transfer to the surrounding medium as well as the heat transfer in the material. The heat (temperature) and the structure (deformation) is uncoupled, meaning that deformation is calculated based solely on the temperature, but the heat generated by plastic yielding is neglected. It is possible that the temperature field is influenced by the deformation rate but it is almost always neglected. The distortion is calculated in every node of the mesh. The model considers the sequence in the calculation. It is a full transient model simulation meaning that it is carried out time dependent and all steady-state parameters are replaced by a transient parameters set, taken every time step into account (Lorin, 2015).

How the part deforms due the heat application is also affected by the positioning system of the part. The purpose of the positioning system is to lock the part in six degrees of freedom, three translations and three rotations (Robust Design & Tolerancing, 2014). This location scheme will define how the forces act and the reactions they will get on the part.

4.1.2 The FE Model and RD&T

The geometrical model used in the simulation comes from a CAD model of the A-pillar, which is the same as in the physical tests. The model is a surface mesh that is composed mostly of hexahedral elements. It includes three different element sizes to reduce simulation time while simultaneously obtaining accuracy in fundamental areas of the part. Figure 26 shows different colour coding for each element size of the part´s mesh. The flanges of the part (yellow) have the smallest element size, 4 mm; the middle part (blue) has 6 mm; and the top area of the part has 10 mm. The mesh was created in the software, Femap .

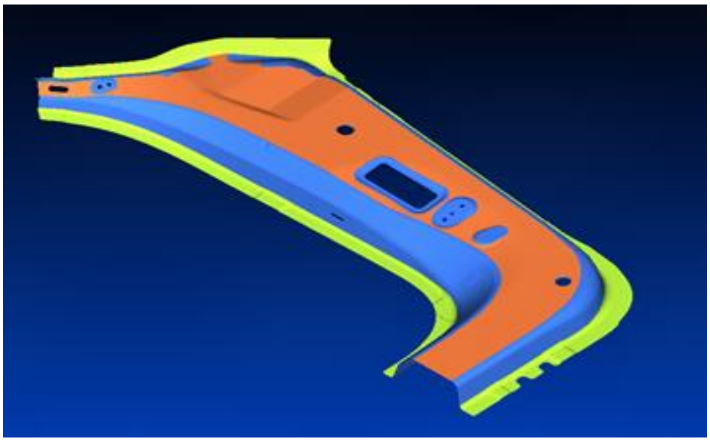

Figure 26: FEM mesh sizes

The point description used in the simulation differs from the one used in the physical tests. The total amount of points is 27 with 80 mm distance between each of them. The part is locked by using a 6-directions positioning system (non-orthogonal directions) where six points in three directions are positioned in four different placements of the part (Figure 27). The placement one locks the part in Y- and X directions, placement two locks it in Y- and Z directions, placement three in X-direction, and placement four in Y-direction.

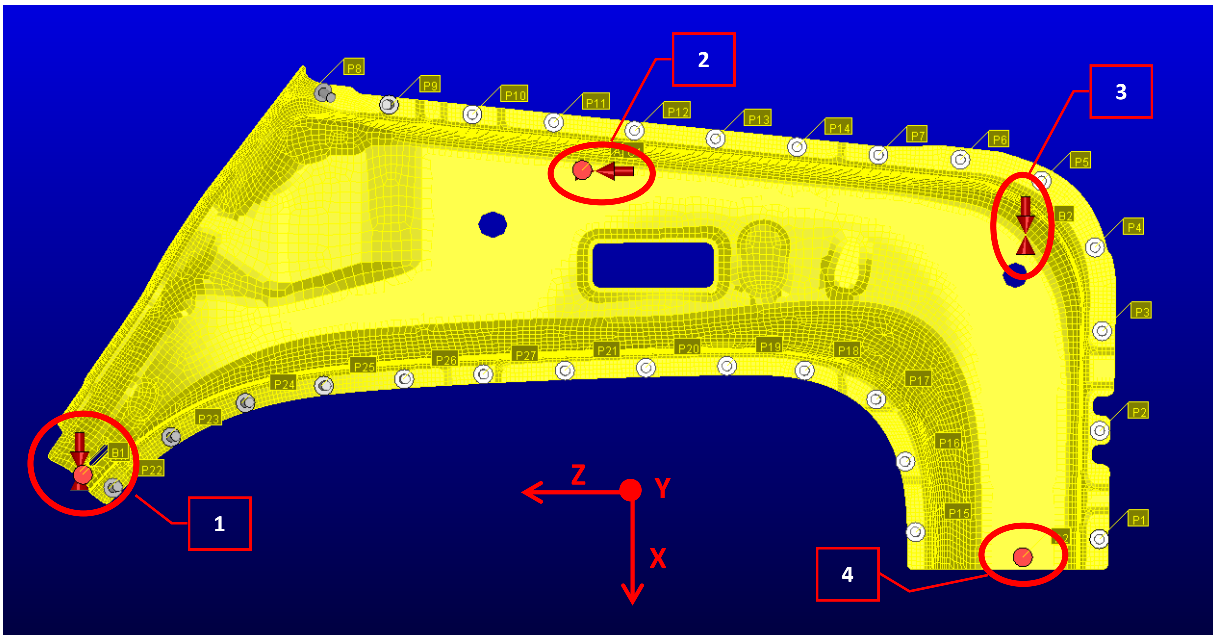

Figure 27: A-pillar model with sequence A and 6-direction positioning system

The heat analysis settings can be seen in Table 5. The duration represents the tempering time of each point for which the smallest value was chosen to meet production requirements of low cycle time. The delay value is the time between tempering points and was selected as an assumption of the traveling time of the robot between points. During the physical tests, it was hard to define the laser diameter and it was estimated to be between 1 and 4 mm, and it was therefore decided to go for a value of 2 mm in the simulation. The depth value was decided based on the thickness of the part, with the intention of having the laser applied all the way through. The laser power is from the physical tests with a 100% effect on it.

Table 5. RD&T simulation settings.

Settings	
Duration (sec)	0,5
Delay (sec)	2
Diameter (mm)	2
Depth (mm)	1.6
Power (kw)	1.75
Effect (%)	100

4.1.3 Material Properties

Since the material needed for the simulation is Usibor 1500 in martensitic-phase there is not enough information about it available at VCC. Its properties at room temperature and its chemical composition are the only accessible information. The lack of knowledge of the material properties exists since for thermo-mechanical simulation, it is required to know them through a wide range of temperatures. To get this data, the software JMatPro was used. This software requires the material composition, which taken from Güler (2013), as well as the grain size (Naderi, Uthaisangsuk, Prahl, & Bleck, 2007). This information can be seen as the input for JMatPro in Figure 28. The information for the expansion values was not available in the required format; therefore values from a related material, DP600 steel, were used. The material file can be consulted in the Appendix X.

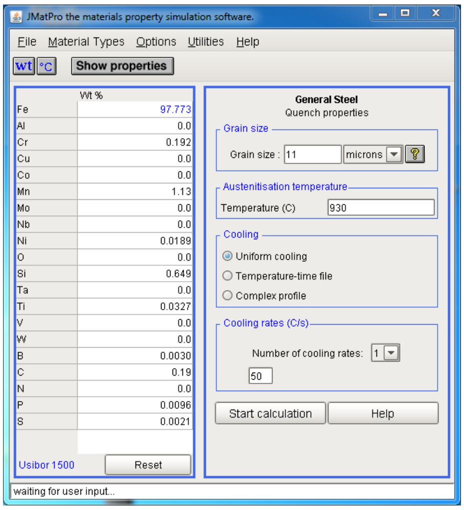

Figure 28: JMatPro settings

4.1.4 Results

The results from the simulation were analysed through the use of the software ParaView. The displacement magnitude for each point was examined. The data for each sequence is composed of 44.591 points, representing the number of nodes, with a number of time steps are 1602.

The colour plots of the deformation (magnitude) at the last time step for all the five sequences show that there is no visible difference between them (Figure 30). All the sequences follow the same deformation pattern, regarding both magnitude and position. Plots of displacement magnitude of all data points for each sequence are found in Appendix XI.

The data was analysed with two different perspectives. First, statistical analysis was made with all data points (Analysis 1) and secondly, critical area of the part was defined and smaller sample was examined (Analysis 2).

Analysis 1

If the results are analysed numerically, a difference is noticed between the sequences. Table 6 shows the maximum, minimum, mean and median values of the data for all the five sequences. The mean value of the sequence data is then compared and plotted in Figure 29. This analysis shows that there is a difference between the sequences. The mean value of sequence B and D vary the most and the difference between them is 2,9 %.

Table 6. Statistical values of each sequence data.

	Sequence A	Sequence B	Sequence C	Sequence D	Sequence E
Max value	0,9357	0,9143	0,9378	0,9543	0,9312
Min value	0,0163	0,0157	0,0161	0,0152	0,0165
Mean value	0,2169	0,2129	0,2171	0,2191	0,2158
Median value	0,1380	0,1356	0,1379	0,1414	0,1369

Figure 29: Colour plots of the deformation at the last time step for all the simulated sequences

Sequence A

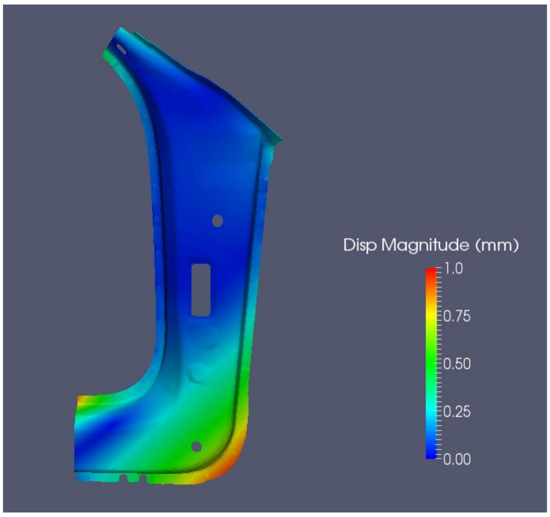

Sequence B

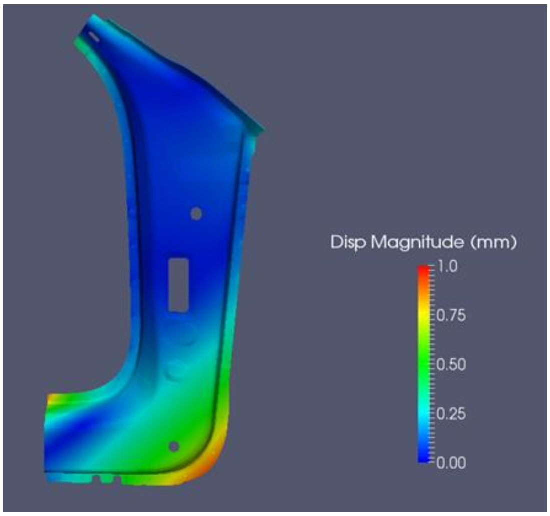

Sequence C

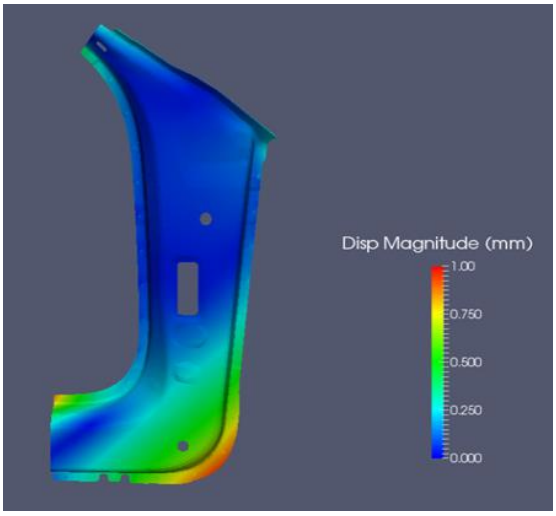

Sequence D

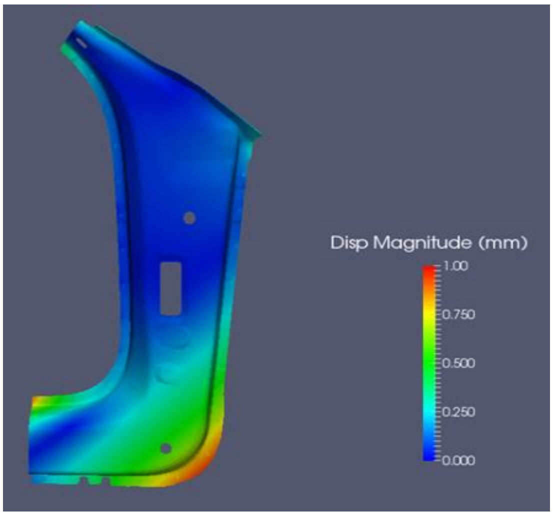

Sequence E

Figure 30: Displacement analysis; the mean value of each sequence data

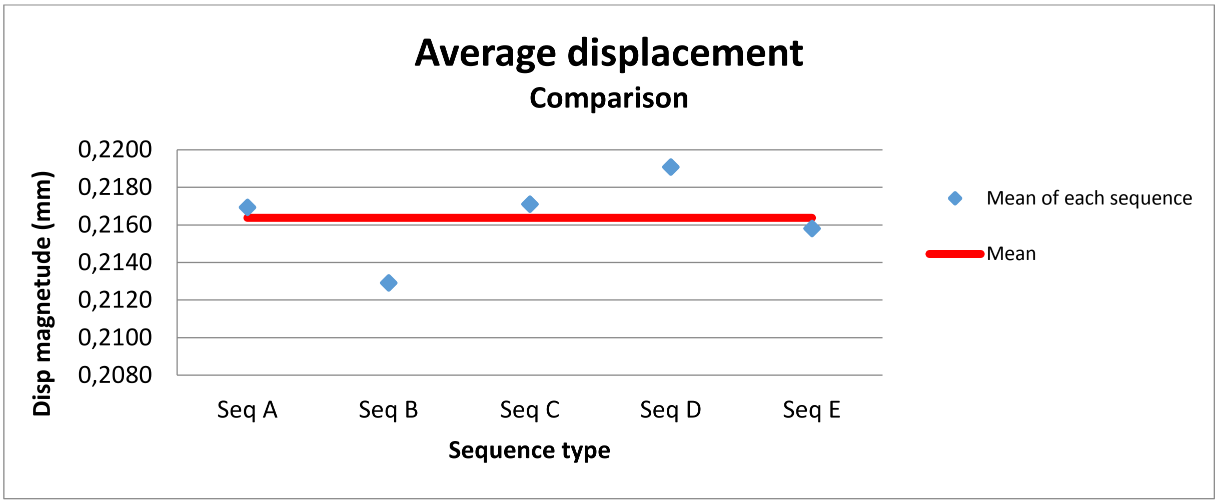

Analysis 2

It is important to investigate the data with different analytical perspectives in order to validate the results. Comparing the whole data of each sequence does not comprehend all aspects of the part's deformation. For example, there can exist an area on the part where the deformation pattern between the sequences contrasts the results from the analysis one.

It was decided to look further into the area of the part where the most deformation occurred, called critical area. Random line of data was selected from the critical area, including 369 points (Figure 31). Mean values were calculated for each point in the data and plotted (Appendix XII). Furthermore, to improve the visualization of the data a new sample, of twenty points, was chosen from bigger one and plotted (Figure 32). The small sample (20 points) is a subset of the critical area of the larger sample (369 points).

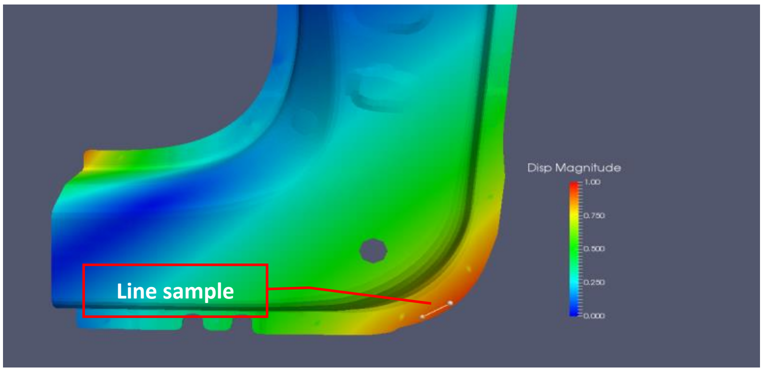

Figure 31: Critical area of the part including new sample line

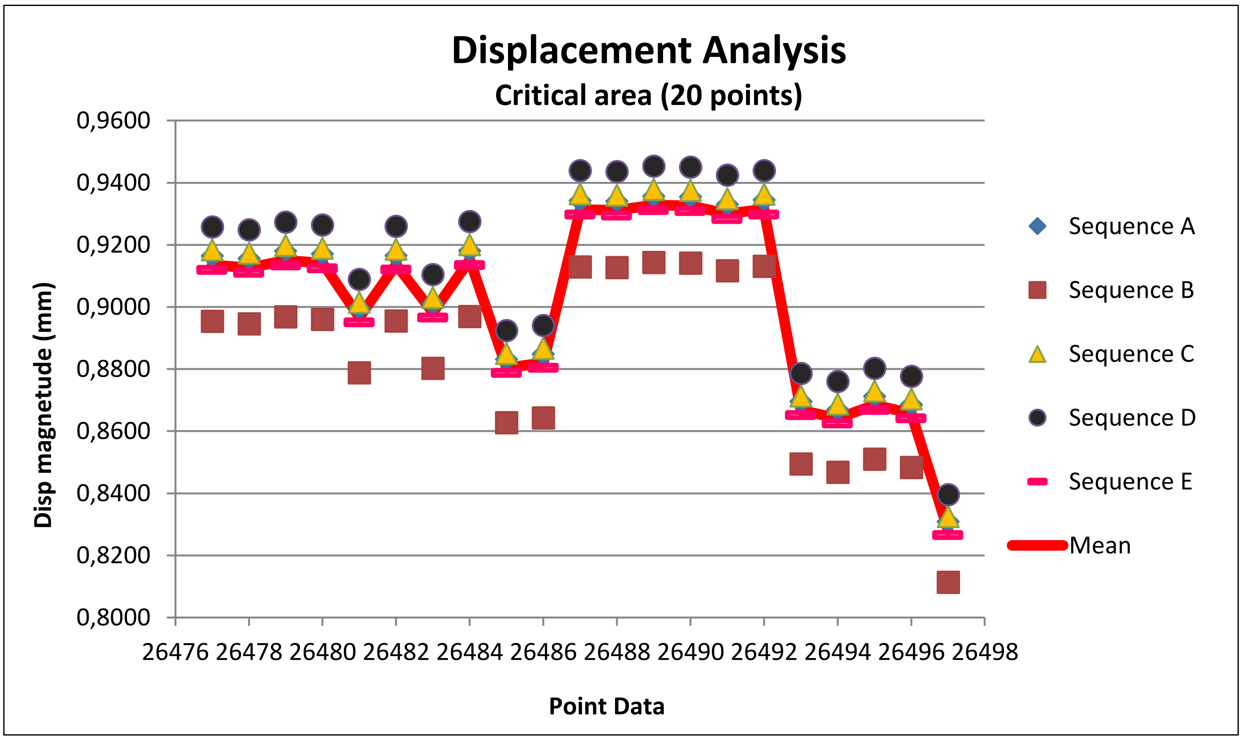

Figure 32: Displacement analysis; control limits of each point data, belonging to critical area

The Analysis 2 gives the same statistical results as in Analysis 1. As seen in Figure 32, both sequence B and D varies the most while the other three sequences lie around the mean value. The numerical difference between points B and D is in average 3,42 %.

4.2 Physical Tests

The physical tests have the main objective to verify the results from the simulation. Volvo Cars provided eight A-Pillars for this stage. The first step was to 3D-scan them to know their exact geometry before the laser tempering. The next step was to apply the laser sequences developed for this purpose and then 3D-scan them again.

On the physical parts, 35 points were selected. They have an even distribution among them, but are closer in the areas where, as suggested by Hansson (2015), the part will concentrate more energy in case of a collision. Figure 33 shows the marked points on the A-pillar.

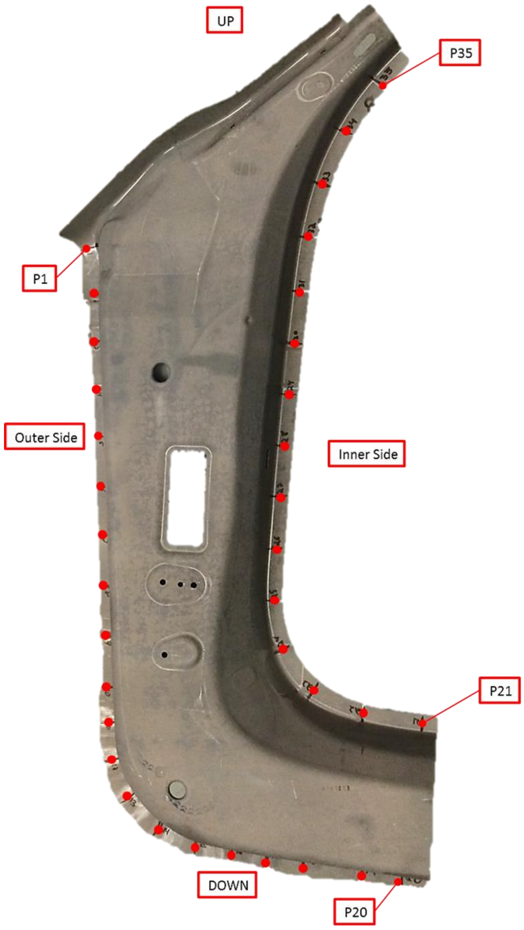

Figure 33: Physical test tempering points

Since there were only available 8 A-Pillars for physical testing, only four sequences were selected. The intention was to try four sequences twice each. For this, sequences A, B, C and D were selected. However, nothing can be concluded since the results for these tests were discarded for the following reasons:

- The laser used was Laserline LDF 4000-60, which is different to the one used before by Swerea and VCC, and the one used in Temperature & Hardness Tests section. Due to lack of experience with this laser head, too low power was used during the testing so the reflecting hardness drop in the part was not sufficient enough for the SPR process.
- The parts were stored for a long time, period in which the residual stresses affect the geometry and material changes occur.

4.3 Conclusion of the sequence study

There is a relation between the tempered points sequence and geometrical deformation. This has been proved through simulations but it needs to be verified thoroughly with physical tests. The simulation manifested small numerical difference between the sequences, of approximately 3%, but as the simulation did not include residual stresses nor a proper material module in its heat analysis module it is hard to conclude how the part will react from physical tests. However, it can be stated that thermal expansion causes geometry deformation when a laser is used to temper the part.

It is hard to predict the pattern of sequence that will provide the minimum deformation only from the five simulated sequences. Figure 34 illustrates the deformation level of the sequences' result, from the smallest deformation (sequence B) to the largest (sequence D). One theory is that when heat is applied in a sequence, from inside to the outside of the part's flange, the forces created, or gauss points between the elements, move outwards with less reaction forces. This causes less plastic strains, which later are considered as part deformation. More sequences need to be simulated for optimization purposes, in order to make a conclusion.

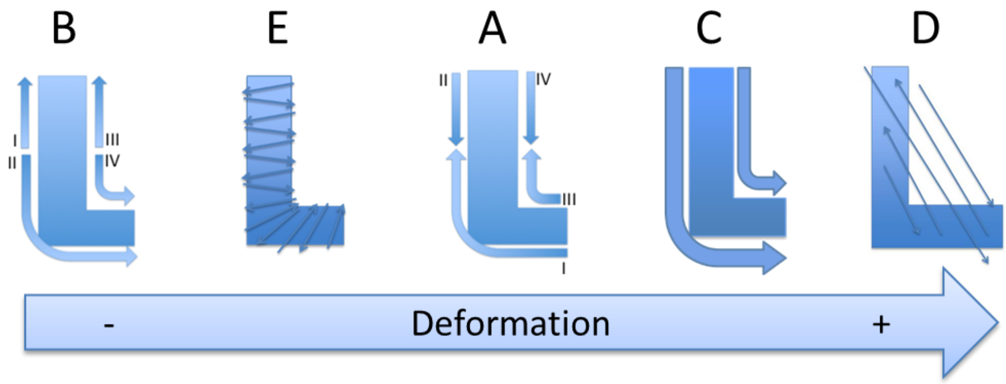

Figure 34: The deformation order of the sequences, smallest to largest.

5. Discussion

5.1 Goal 1 - Ranking of factors affecting geometrical impact for the case part

The main causes of deformation during heat treatment are thermal expansion and release of residual stresses but regardless of that, the existence of the residual stresses in a hot stamped part made of boron steel has often been questioned in the industry. As an example of this, the material vendor, in this case ArcelorMittal, claims that parts made of this material by hot-stamping have absolutely no spring-back.

The interest of stakeholders, such as boron steel producers, are enormous resulting in deceptive information in literature that often can be questioned. When investigating matters like this, it is important to discuss with different stakeholders and get different perspectives. The problem is though that different stakeholders have often difficulty to share information, which makes it harder to investigate.

The study of the literature and the discussion of different experts and stakeholders regarding geometrical impact of heat treatment was considered successful and adequate. It gave a comprehensive understanding of the issue and important foundation for further study of the matter.

5.2 Goal 2 - Establish the laser parameters to get the optimal hardness for self-pierce riveting

Results from the laser tests show that higher laser power results in higher temperature, consequently, and that gives softer material and bigger deformation. However, these tests were done on a thin sheet of metal of 1 mm. The A-pillar, for example, is 1.6 mm, and the knowledge acquired from the laser testing have to be validated for thicker parts and different geometries. Future tests must prove that same laser settings can be applied to the A-Pillar.

In contrast to what is recommended in a relation to diminish the distortion, lower hardness and hence higher energy input to the part can improve the SPR process, e.g., less energy consumption and longer tooling life. Consequently, it is proposed that the hardness level of the material gets optimized with respect to all aspects of the production processes.

It was realised later in the thesis work the importance of investigating the laser parameters. It was thought that the laser parameters established could be applicable on other laser heads but that was not the case because they behave differently.

To be able to compare different results when tempering, accurate and high quality working procedure must be established. As seen from the physical tests of the sequences in chapter 4, optimizing laser parameters for laser tempering is advised to gain full control of the process. Manufacturing variances are already existing between the parts so the variances in the tempering process need to be reduced.

5.3 Goal 3 - Define the relation between laser sequence and deformation

The previous goal proved that root causes of distortion during the tempering process are thermal expansion and release of residual stresses. However, the magnitude and the position of the residual stresses in the part are unknown, which makes it hard to predict how much influence their release has in comparison to the deformation caused by thermal expansion.

The residual stresses could have considerable impact on the geometry, compared to heat expansion, and that they need to be included in the thermal simulation tool to give significant results. On the other hand, the residual stresses might also not impact the deformation in such a big manner that they have to be included. Meaning that heat expansion is the vital factor for deformation when point tempering the A-pillar.

To test the impact of residual stresses further physical tests along with simulation of different sequences needs to be done. A proper plan for physical tests is required to minimize all variances in the process. Three different scenarios of results from the comparison is interesting to analyse.

1. Physical tests give different deformation magnitude and pattern then simulation. The physical tests and the simulation give same results regarding the sequence optimization.
2. Physical tests and simulation give the same results regarding both deformation magnitude, pattern and sequence optimization.
3. Physical tests and simulation results give different results regarding both deformation magnitude, pattern and sequence optimization.

Scenario one confirms that residual stresses are not necessary when simulating the optimal sequence. If the displacement pattern in this scenario is identical for both testing tools but not the magnitude it shows that residual stresses only magnify the distortion in the part and it might be possible to create a calculation model to predict that. However if the magnitude is the same but the pattern is not, than residual stresses impact how the thermal expansion affects the part and its structure.

Scenario two confirms that residual stresses do not impact deformation and it is adequate to take only thermal expansion into consideration when simulating the tempering process. Last scenario will on the other hand state the opposite. Residual stresses, their position and magnitude, are the main impact factors for causing deformation in the A-pillar during tempering process.

The goal three was partially fulfilled because the relation of sequence and deformation was only established with simulation of the tempering process and not with physical tests, as initially planned. To verify the relation, physical tests are recommended along with the simulation and further development of the simulation tool should be done to improve the reliability of it.

5.4 Goal 4 - Development of simulating tempering process

Regardless of the impact of residual stresses, in order to improve the simulation of the tempering process it is necessary to have correct material data of boron steel through each temperature step in the tempering process and include residual stresses in the model.

The material data was not available when starting the thesis work; neither Swerea nor VCC possessed this information. The material properties used in the thesis were obtained from a simulation tool, called JMatPro, and might not be fully reliable. The material properties have to be tested through a range of temperatures: linear elastic behaviour, thermal conductivity, specific heat, density, and the classic metal plasticity model. Additionally to this, JMatPro expressed the thermal expansion coefficient as an average value (secant) instead of instantaneous (tangent), which is the coefficient that the tempering simulation accepts. A conversion of the coefficients was not available; therefore it was decided to use the thermal expansion coefficient (in an instantaneous form) from DP600.

According to simulation experts it is possible to include position and magnitude of residual stresses into the simulation, however the main difficulty is to map them from physical parts. That can be done with high level of difficulty, through physical tests and through simulation. To be able to conduct accurate simulation to map the residual stresses a good material model and part model is required.

A good material model includes all the material properties through a set of different temperatures, including the material phase changes from austenite to martensite that occurs during hot stamping. These properties will define the behaviour of the part itself, describing the residual stresses. To get the information requires time, which during this thesis work is not possible.

A good part model takes all the factors that create residual stresses into consideration. The residual stresses can change from part to part, and even small differences in geometry can completely change their appearance. All manufacturing processes create residual stresses in the part, due to thermal and mechanical operations in it. Apart from the hot stamping, the A-pillar goes through other processes such as blanking, trimming, and flanging that are performed both before and after the hot stamping. These processes affect the part's geometry, both by creating new residual stresses in the material and by altering the existing ones. This has to be taken into account for future studies.

5.5 Synopsis

During the thesis work it was realised that the topic was broad and that it included unexplored areas within material – and simulation technology. A lot of crucial information related to the thesis work was expected to be available within VCC but was not.

The reason why VCC has not simulated the hot stamping process and gathered the required information in this matter is due to its complexity and to the fact that it has been unnecessary.

The boron steel parts used to be mainly produced by suppliers, but it is now that VCC is focusing on producing them in-house. When buying and/or producing these parts, VCC was mostly concerned about meeting the production requirements. Additionally, their main focus regarding simulation of boron steel was done by the crash test division, which are done at room temperature. Everything mentioned before contributes to the big gap in knowledge of hot stamped boron steel parts, like the A-pillar, inside the organization.

At the end, it is up to VCC to obtain the missing knowledge required to develop the tempering process and boron steel technology. The opportunities that the tempering process provides are wide-ranging and apply to many other mechanical operations besides SPR. The application of boron steel is starting to be more common inside the automotive industry, with its properties becoming vital to meet demands in today's environmentally aware society.

6. Recommendations

6.1 RD&T

One of the main drawback of RD&T is the lack of an indicator of what it is doing and if it is encountering errors. While the simulation is running, the software becomes irresponsive. During the thesis work, a lot of time was wasted because RD&T did not give any feedback of the simulation status, and often it presented error message in the log file after some hours of running, just to later realize through the log that it had been failing from the beginning. The only way to understand that it is actually doing something and not crashing is to go to the log file that is created. This would not be user friendly, since there is no explanation of the things displayed in it; if the goal is to develop a general-user software that needs to be improved. However, in the case of the thesis work, good access to the developers for support was possible, that will not necessary be the case for future users.

For inputting the sequences to the software was a fairly easy task. What can be improved though, is the visual relation of the point information in the Heat Analysis interface with the points shown in the CAD part. It would be easier if there is a way to name the points at convenience, or even adding them into a table, in which it were possible to just drag them into a desired order. In this interactive table, it would also be possible to input the laser parameters settings without having to go to the text boxes below and clicking apply.

The summary of the recommendations of RD&T is listed below.

Table 7: RD&T recommendations.

1.	Improve the simulation by including residual stresses.
2.	Clarify the units used in the material file.
3.	Match the Heat Analysis settings with the real tempering tools.
4.	Quality mesh feedback from the software.
5.	Upgrade functions in the Heat Analysis module.
6.	Allow free positioning system.
7.	Show the simulation time, progress time and status.

8.	Error explanation.
9.	Better point name system.

1. The input model should include residual stresses. RD&T allows to do Heat Anlysis on a mesh that contains residual stresses. This can be obtained by physical tests, or more conveniently through hot stamping simulation.

2. About the material file, the units to be used were not clearly specified. The recommended units were SI units as used in ABAQUS, but it was not consistent. Just a clear specification of the units to use.

3. The parameters used in the Heat Analysis module of RD&T must match the ones from real tempering tool, the laser. For example, the laser settings for power and effect should heat the part to the same maximum temperature as in the physical tests. Also, it would be useful to have the option to put maximum temperature and not power as an input.

4. Add the functionality to the software to verify the mesh quality. Additionally, clarify which type of mesh is more convenient to use, e.g., hexahedral or tetrahedral.

5. Upgrade functions of the Heat Analysis module, by adding the hardness target, as a function of temperature. Information from the coupons tests can be used to develop this upgrade feature. By this, it would be possible to relate the temperature and the consequent change in hardness.

6. The positioning system has an impact on the result. Therefore it is recommended to include positioning system that allows the part to move freely, as if it was placed without any clamps or fixture, like just over a table.

7. Show the simulation time and percentage during simulation. Differentiate when the software is crashing and properly running.

8. An explanation of the error messages about why it went wrong. A list of the possible errors, its explanations and possible solutions is advised.

9. Have better interface of the numbering system in the heat analysis, even opening the possibility of naming the points at convenience, or having them organized through and interactive table.

6.2 Thesis Research & Future Work

Table 8: Thesis recommendation

1.	Get the material data at different temperatures.
2.	Test the definitive laser on the right part with the right thickness.
3.	Optimize the laser settings relative to the required hardness.
4.	Testing the impact of residual stresses on deformation.
5.	Optimize the sequence of tempered points in the A-pillar.
6.	Develop a universal methodology to find the optimal sequence.
7.	Optimize the part production process to decrease the residual stresses.
8.	Studies on welding quality by implementing tempering prior to the welding process

1. Investigate the real material properties through a range of different temperatures. This is also a recommendation required for RD&T, but since it will also apply to any hot stamping simulation, it is a recommendation for the whole thesis.

2. Test the laser parameters better according to the exact laser type that will be in the production. Parameters should be tested with the exact material and geometry, including different thicknesses.

3. Optimize the laser settings relative to the required hardness, the resultant distortion, tool life, or energy consumption.

4. Test how much residual stresses impact the deformation, in a relation with thermal expansion, by comparing results from simulation and physical tests.

5. Optimize the sequence of tempered points in the A-pillar by using the required tools and knowledge gained from earlier recommendation.

6. Universal method for establishing the optimal sequence for minimal deformation needs to be done. Such a method will be able to find the best sequence independently of the part’s geometry, material, tempered points, etc. Additionally, future tests with the same part (the A-pillar) but different material is advised as a way of confirming the validity of the selected sequence and even of the universal method.

7. Since additional operations create residual stresses, the order of them respective to the hot stamping process has to be thoroughly analysed.

8. When welding, the part could not be only deforming because of it is being fixed, but also to thermal expansion, phase changes, and residual stresses being released.

Further studies on improving the welding quality by using the technology of tempering process are advised.

7. Summary & Conclusions

7.1 Summary

The thesis work started with the goal of finding the causes of geometrical deformation after laser tempering a boron steel A-Pillar. The importance of reducing the distortion comes from the need to improve geometrical assurance during all engineering activities. Finding out the root causes of the distortion will help to predict it and to discover ways of counteracting their effects. Boron steel is used in the automotive industry due to the demands for lighter and safer vehicles. When new materials or technology arrive to market, they pose new and unknown challenges, but a wide range of opportunities. There are many unexplored details about boron steel, and one extensive area regarding the material is mechanical joining, and more precisely the joining of boron steel and composites material. The combination of these two materials, among other lightweight materials, represents the future of the automotive industry towards lighter and consumption efficient vehicles.

Boron is an ultra-high strength material that needs to be softened in order to meet the requirements posed by the self-pierce rivet process. The laser applies energy to concentrated area in the material to change its hardness. Other material properties get affected during the process, such as reduction in yield – and tensile stress. The process includes secondary effects such as thermal expansion and the release of residual stresses, which result in deformation. Thermal expansion and the non-uniform release of residual stresses are known factors for being the root causes of distortion during heat treatment, of any kind.

The thesis investigates prior production processes of the part along with studies of welding processes of the same material, both to understand the part's material properties and its behaviour. According to literature study and consultation with experts, it can be stated that the A-pillar made of boron steel and formed by hot-stamping process has residual stresses.

According to research done on 'optimal welding sequences to minimize distortion' of boron steel part, it is explained that the part experiences distortion due to the applied heat and that it is being fixed into a position. During the welding process, new stresses are generated in the fixture of the part, residual stresses are being released, phase changes and thermal expansion occurs. These phenomena cause deformation.

Another gap in the study of the tempering process was optimizing the laser parameters to gain sufficient hardness in the material and additionally minimizing the energy input in the part. There was a vague idea of the ideal hardness for the SPR, but no information of the amount of temperature needed to reach that hardness and the right laser settings required to create that temperature. After some research and testing, 300 HV was decided as the ideal hardness to have. Different trials were made with the laser, to meet the required hardness value.

Do investigate the relation between laser sequence and deformation, the tempering process was simulated with RD&T. The simulation of different sequences generated different deformations in the part. The difference was small but within numerical tolerances of the model and thus valid. The deformation calculation in the heat analysis model is only based on the heat (temperature), how it transfers in the material and affects the structure. It does not consider the existence of residual stresses in the part. According to the simulation results, the sequence has an effect on the geometry taking only thermal expansion into consideration and therefore it proves that there is a relation between a sequence and deformation. The existence of residual stresses in the A-pillar is known and when those residual stresses are released non-uniformly during the tempering process they cause distortion in the part. However their exact effectiveness on the distortion compared to heat expansion is still unknown.

7.2 Conclusion

1. The factors that influence the parts deformation are the existence of residual stresses, thermal expansion and phase transformation.
2. On a 1 mm boron steel coupon, the ideal hardness of 300 HV is reached at 745°C, i.e., 1.75 kW at 0,5 seconds.
3. Simulation of the tempering process in an A-pillar proved that there is a relation between sequence and deformation in the part, taking only thermal expansion into consideration. The sequence that proved to cause least distortion in the part is the one that aimed to create the forces towards the outside of the part. This needs to be verified in physical tests.
4. The most important factor of improving the accuracy of the simulation of the tempering process is the insertion of the initial residual stresses in the RD&T simulation. Regarding RD&T functional improvements of its interface, the major part missing was an indicator of the simulation status, and a better way to input the point's information and order.

References

Altan, T., & Tekkaya, A. E. (2012). *Sheet metal froming, process and applications.* Ohio: ASM International.

ArcelorMittal. (2014, January 28). *Steels for hot stamping - Usibor®.* Retrieved from Automotive Worldwide: http://automotive.arcelormittal.com/saturnus/sheets/E_EN.pdf

Automotive Steel Definitions. (2015, February 9). *Automotive steel definitions*. Retrieved from WorldAutoSteel: http://www.worldautosteel.org/steel-basics/automotive-steel-definitions/

Baltazar Hernandez , V. H., Nayak, S. S., & Zhou, Y. (2011). Tempering of Martensite in Dual-Phase Steels and Its Effects. *The Minerals, Metals & Materials Society and ASM International, 42A*, 3115-3129.

Berglund, G. (2008). The history of hardening of boron steel in northern Sweden. *In: 1st International Conference on Hot Sheet Metal Forming of High-Performance Steel*, (pp. 175-177). Kassel, Germany.

Bhadeshia, H. (2015, February 10.). *Tempered Martensite*. Retrieved from University of Cambridge: http://www.msm.cam.ac.uk/phasetrans/2004/Tempered.Martensite/tempered.martensite.html

Bhat, S. (2011, May 18). *Advances in High Strength Steels for Automotive Applications*. Retrieved January 28, 2015, from Autosteel Web site: http://www.autosteel.org/~/media/Files/Autosteel/Great Designs in Steel/GDIS 2008/12 - Advances in AHSS for Automotive Applications.pdf

Callister, W. D. (2007). *Material schience and engineering; an introduction.* New York: John Wiley & Sons, Inc.

Drossopolu. (1996, May 28). *Genetic Algorithms.* Retrieved from Imperial College London: http://www.doc.ic.ac.uk/~nd/surprise_96/journal/vol1/hmw/article1.html

Frydman, S., & Letkowska, B. (2012). *Properties of Boron Steel After Different Heat Treatments*. Retrieved January 28, 2015, from International scientific journarl: http://mech-ing.com/journal/Archive/2012/9/84-frydman_mtm12-paper_expanded.pdf

Furuhara, T., Kobayashi , K., & Maki, T. (2004). Control of Cementite Precipitation in Lath Martensite by Rapid. *ISIJ International, 44*, 1937-1944.

Gildea, D. (2004, October 28). *Greedy Algorithms.* Retrieved February 16, 2015, from University of Rochester: https://www.cs.rochester.edu/~gildea/csc282/slides/C16-greedy.pdf

Güler, H. (2013). Investigation of Usibor 1500, formability in a hot forming operation.

Hansson, S. (2015, April 21). (public communication). *Volvo Car Corporation*. Olafström, Sewden.

Hansson, S. (2015, February 3). Self Piercing Rivets 2015 Plugg. Olafström, Sweden: Volvo Cars Corporation.

Icon, J. C. (2005). *Laser processing of engineering materials: Principle, procedure and industrial application.* Oxford: Butterworth-Heiniemann.

Johnson , D., & McGeoch, L. (1995, November 20). *The Traveling Salesman Problem: A Case Study in Local Optimization.* Retrieved from KTH Web site : http://www.csc.kth.se/utbildning/kth/kurser/DD2440/avalg14/TSP-JohMcg97.pdf

K., W., R., S., & L., L. (2010). Strategies for optimization of sport welding with respect to geometrical variation in sheet metal assemblies. *Proeccedings of the ASME 2010 international mechanical engineering congress and exposition.* Vancover: IMECE .

Karbasian, H., & Tekkaya, A. (2010). A review on hot stamping. *Journal of Material Processing Technology, 210*, 2103-2118.

Key to metal. (2007, Novmber). *Boron in steel: Part 1*. Retrieved from Key to metal: http://keytometals.com/page.aspx?ID=CheckArticle&site=kts&NM=212

Key to metal. (2015, February 10). *The tempering of martensite: Part one*. Retrieved from KEY to METALS Web site: http://www.keytometals.com/Articles/Art127.htm

Kim, C., Kang, M., & Park, Y. (2011). Laser welding of Al-Si coated hot stamping steel. *Procedia Engineering*.

Klarreich , E. (2013, January 30). *Computer Scientists Find New Shortcuts for Infamous Traveling Salesman Problem | WIRED*. Retrieved February 16, 2015, from Wired : http://www.wired.com/2013/01/traveling-salesman-problem/all/

Lorin, S. (2015, May 22). (personal communication). *Chalmers University of Technology* . Sewden.

Materia, T. (2007, November). *Boron in Steel*. Retrieved January 28, 2015, from Total Materia: http://keytometals.com/

Merklein, M., & Lechler, J. (2006). Investigation of the thermo-mechanical properties of hot stamping steels. *Journal of Materials Processing Technology*, 452-455.

Merklein, M., & Lechler, J. (2008). Determination of material and process characteristics for hot stamping processes of quenchable ultra high strength steels with respect to a FE-based process design. *SAE World Congress: Innovations in Steel and Applications of Advanced High Strength Steels for Automobile Structures*, (pp. Paper No. 2008-0853).

Naderi, M. (2007). *Hot stamping of ultra high strength steels.* Aachen: RWTH Aachen.

Naderi, M., Uthaisangsuk, V., Prahl, U., & Bleck, W. (2007, July). A numerical and experimental investigation into hot stamping of boron alloyed heat treated steels. *Steel Research International , 79*(2), 77-84.

Packard, K. (2012, June). *The Fabricator*. Retrieved May 28, 2015, from http://www.thefabricator.com/article/metalsmaterials/metallury-for-welders

PE Geometry Development AB. (2015, January 1). *What is Geometry Assurance?* Retrieved February 11, 2015, from PE Geometry Development AB: http://www.geomdev.se/html/geosakr_eng.html

Pfeifer, M. (2015, Febrary 18). *Residual stress in metal*. Retrieved from Industrial metallurgists, LLC: http://www.imetllc.com/residual-stress-in-metals/

RD&T Technology. (2015, January 1). *The tool RD&T*. Retrieved from RD&T Technology: http://rdnt.se/tool.html

Robust Design & Tolerancing. (2014). *Robustness evaluation and tolerancing analysis: Software manual* (1.16 ed.).

Rosenqvist , M., Falck, A.-C., Lindkvist, L., & Rikard, S. (2014). Geometrical robustness analysis considering manual assembly complexity. *Procedia CIRP, 23*, 98-103.

Sinha, A. K., & Division, B. P. (1991). Defects and Distortion in Heat-Treated. In A. International, *ASM Handbook: Heat Treating* (pp. 601-619). Russel Township: ASM International .

Steen, W. M. (2003). *Laser material processing.* London: Springer-Verlag.

TWI. (2015, March 3). *Techincal knowledge: What is self-piercing riveting and how does it work?* Retrieved from TWI web site: http://www.twi-global.com/technical-knowledge/faqs/process-faqs/faq-what-is-self-piercing-riveting-and-how-does-it-work/

Verlinden, B., Driver, J., Samajdar, I., & Doherty, R. D. (2007). *Thermo-Mechanical Processing of Metallic Materials* . Oxford: Elsevier.

Vinnova. (2012, June 18). *About FFI*. Retrieved February 5, 2015, from Vinnova: http://www.vinnova.se/en/FFI---Strategic-Vehicle-Research-and-Innovation/About-FFI/

Volvo Cars. (2013, December 12). *New Scalable Product Architecture Enables Volvo Car Group to Move Faster Toward a Crash-free Future*. Retrieved from Volvo Cars of North America, newsroom: https://www.media.volvocars.com/us/en-us/media/pressreleases/136653/new-scalable-product-architecture-enables-volvo-car-group-to-move-faster-toward-a-crash-free-future

Wandebäck , F., & Albinsson, O. (2014). *Laseruppmjukning av borstål - Förstudie.* Göteborg: Swerea IVF.

Wärmefjord, K. (2004). *Multivariate Quality Control and Diagnosis of Sources of Variation in Assembled Products.* Gothenburg: Chalmers University of Technology and Göteborg University.

Wärmefjord, K. (2011). *ariation Control in Virtual Product Realization: A Statistical Approach. Gothenburg.* Gothenburg: Chalmers University of Technology.

Webster, H., & Laird, W. J. (1991). *Volume 4: Heat treatment; Martempering - introduction*. Retrieved February 19, 2015, from ASM Handbooks Online: http://products.asminternational.org/hbk/index.jsp

Withers, P. J., & Bhadeshia, H. (2000). Residual stress: Part 1 - Measurement techinques. *Material Science and Technology*, 355-365.

Zhang, C., & Wang, H.-P. (1994). Tolerancing for Design and Manufacturing. In A. Kusiak, *A Handbook of Design Manufacturing and Automation.* Hoboken, NJ, USA: John Wiley & Sons.

Appendix I: Results from tempering tests, chapter 4.1.3

<table>
<tr><th></th><th>Front 1</th><th>Front 2</th><th>Front 3</th></tr>
<tr><td>1000 W</td>
<td>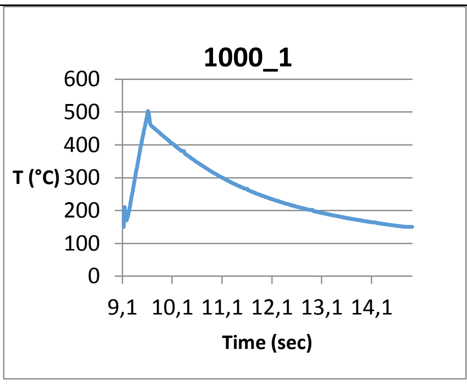
</td>
<td>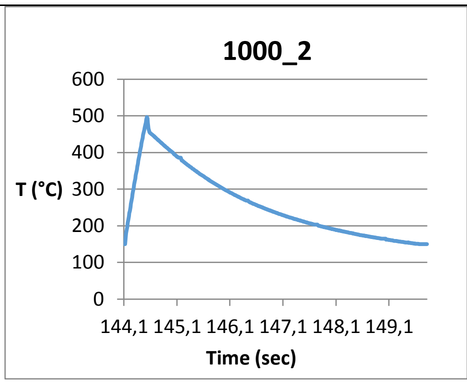
</td>
<td>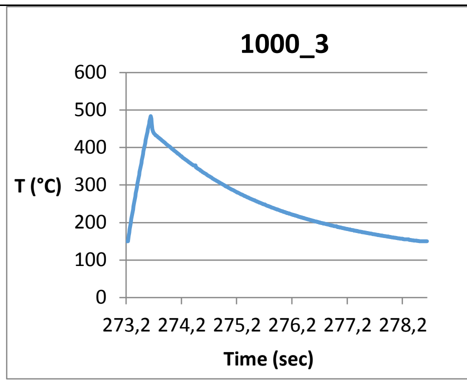
</td></tr>
<tr><td>1500 W</td>
<td>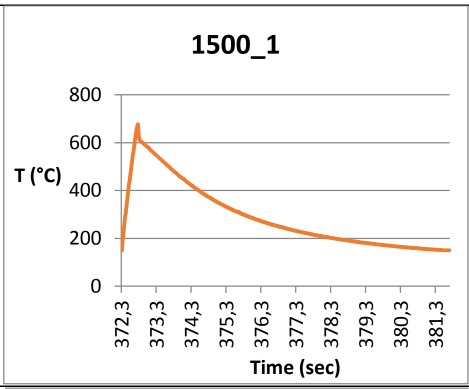
</td>
<td>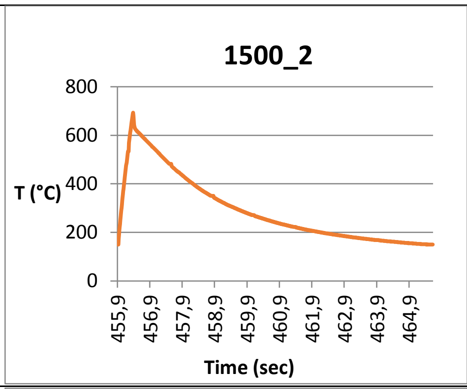
</td>
<td>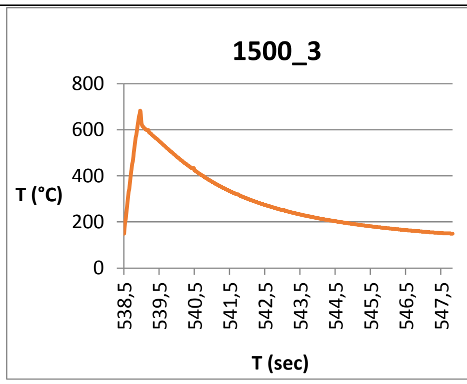
</td></tr>
<tr><td>1750 W</td>
<td>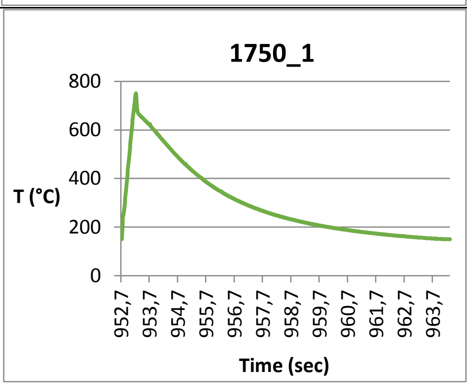
</td>
<td>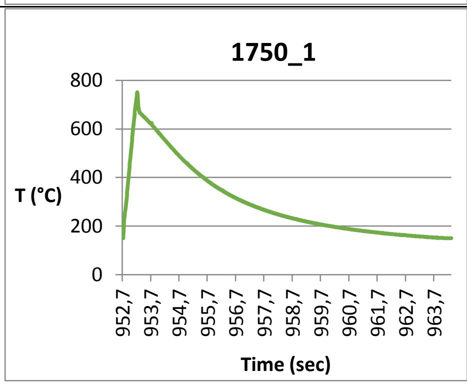
</td>
<td>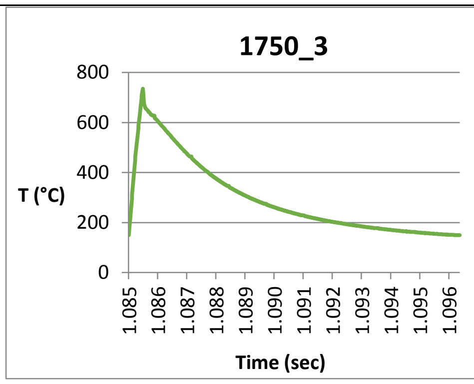
</td></tr>
<tr><td>2000 W</td>
<td>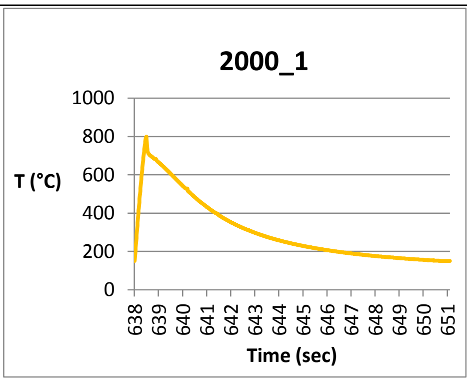
</td>
<td>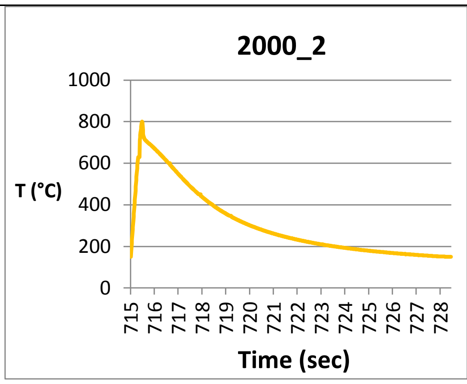
</td>
<td>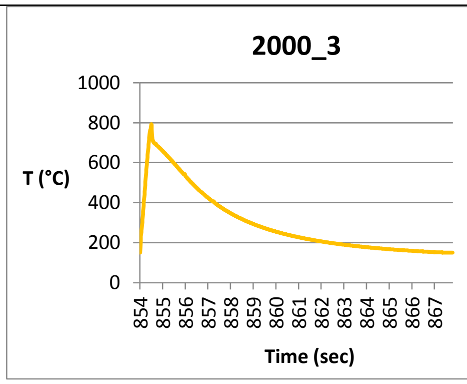
</td></tr>
</table>

<table>
<tr><th></th><th>Back 1</th><th>Back 2</th><th>Back 3</th></tr>
<tr><td>1000 W</td>
<td>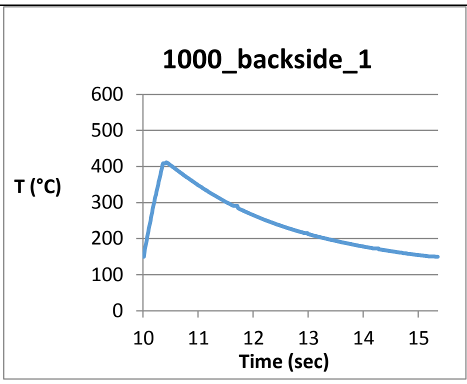
</td>
<td>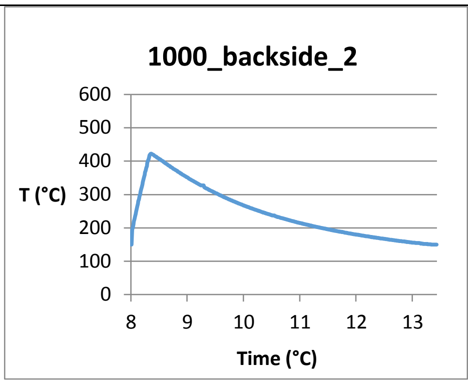
</td>
<td>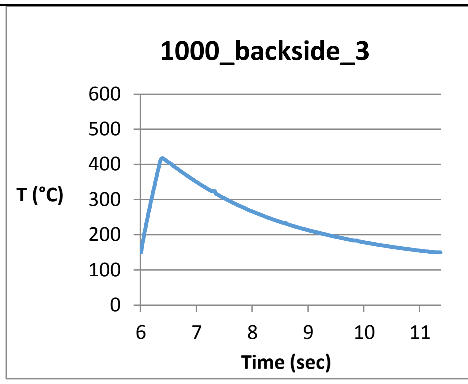
</td></tr>
<tr><td>1500 W</td>
<td>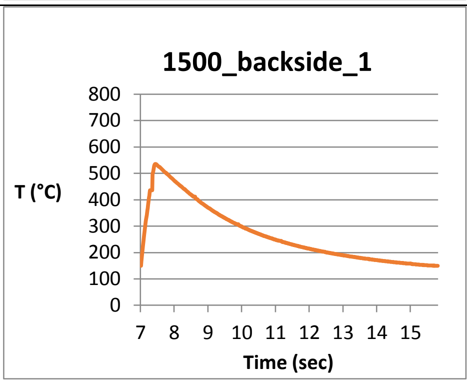
</td>
<td>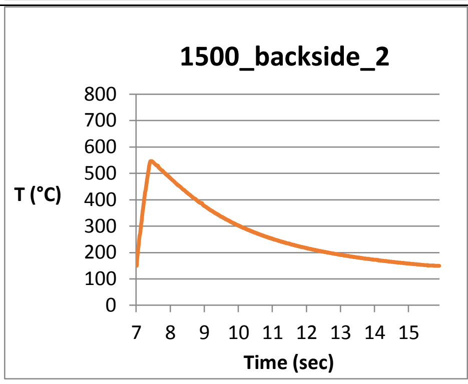
</td>
<td>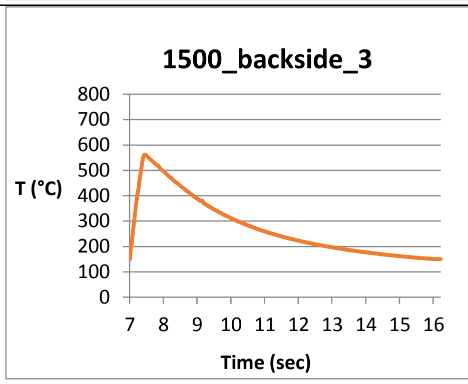
</td></tr>
<tr><td>1750 W</td>
<td>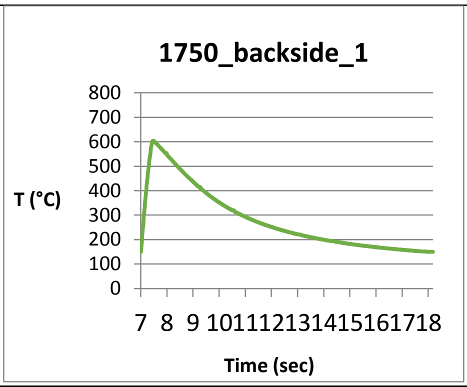
</td>
<td>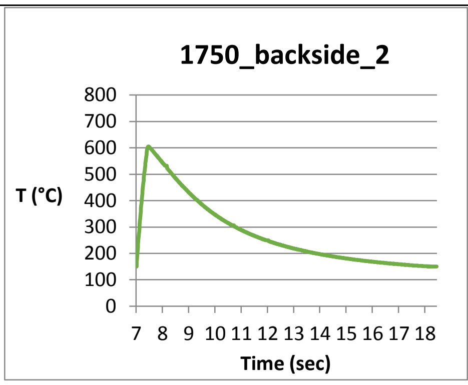
</td>
<td>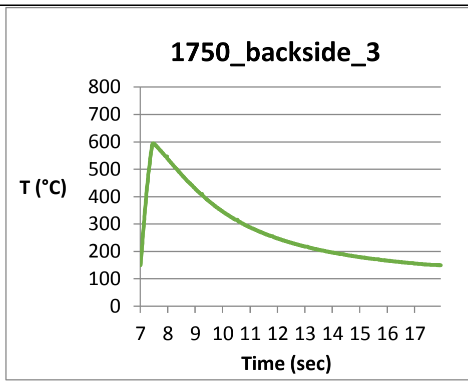
</td></tr>
<tr><td>2000 W</td>
<td>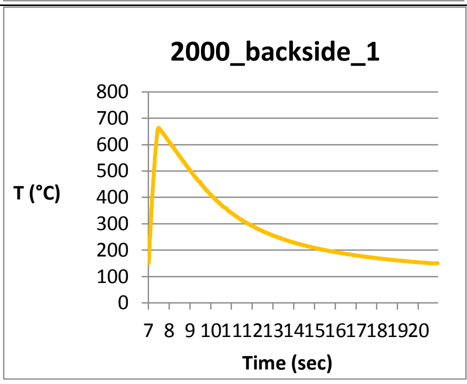
</td>
<td>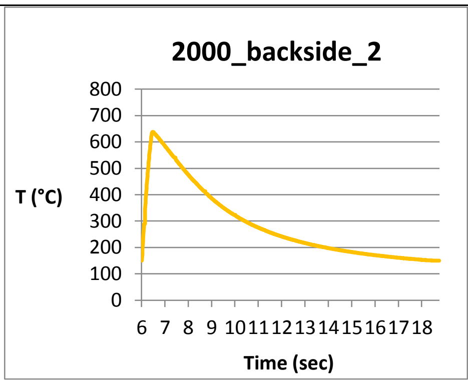
</td>
<td>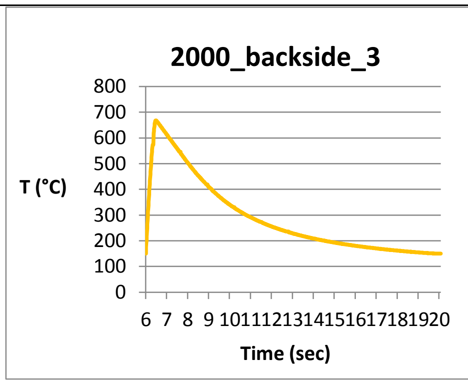
</td></tr>
</table>

Appendix II: Joining description of the spot welded points on the A-pillar, XC90

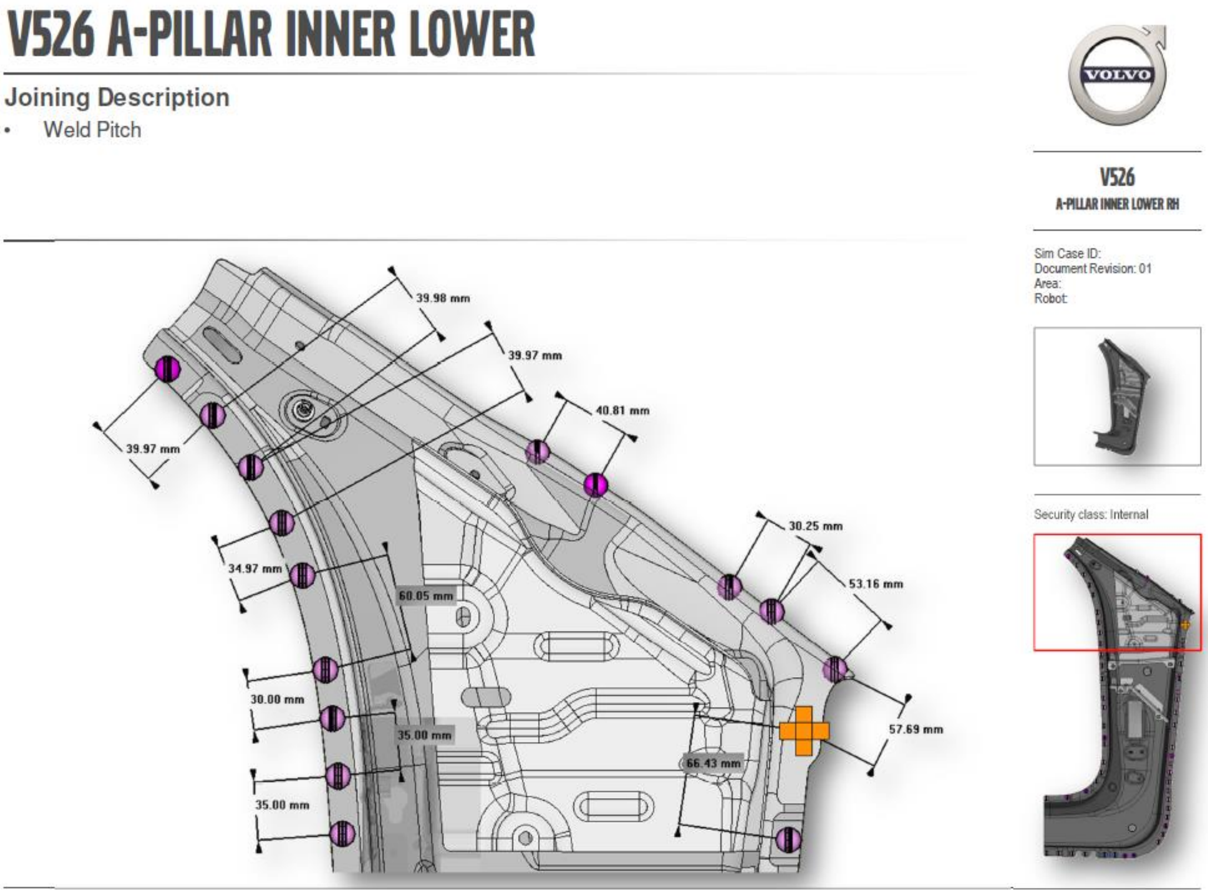

V526 A-PILLAR INNER LOWER

Joining Description

- Weld Pitch

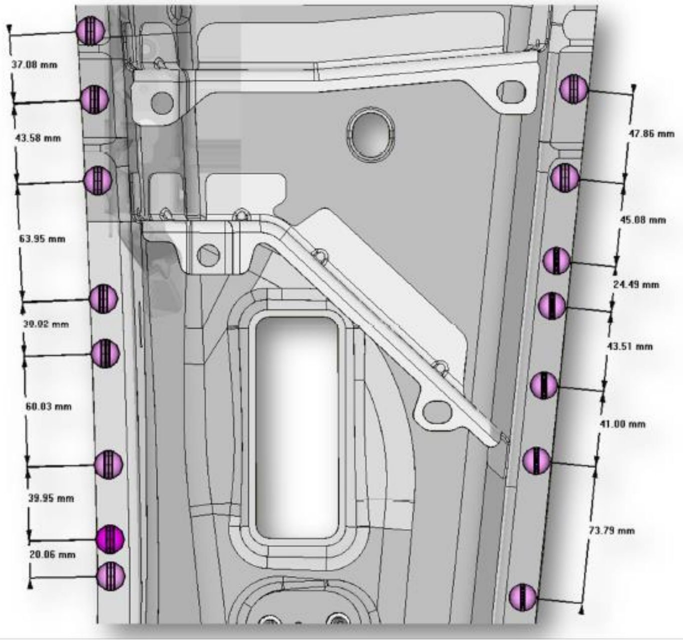

V526

A-PILLAR INNER LOWER RH

Sim Case ID:
Document Revision: 01
Area:
Robot:

Security class: Internal

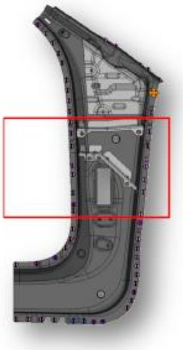

V526 A-PILLAR INNER LOWER

Joining Description

- Weld Pitch

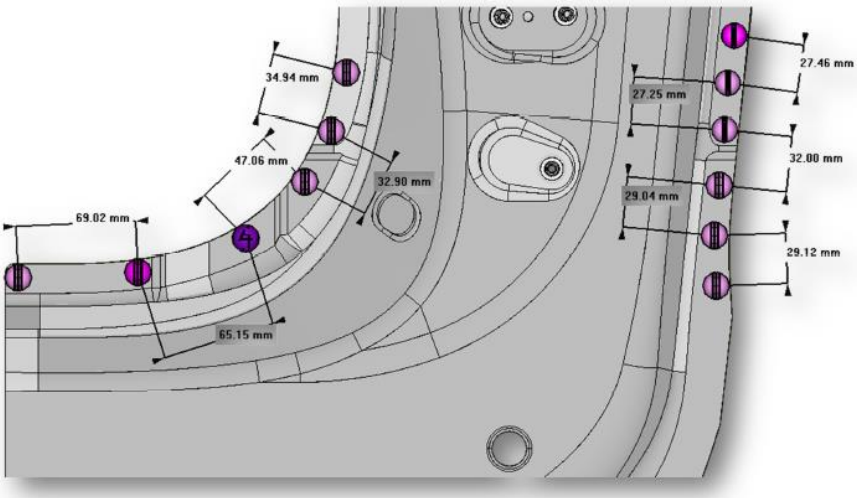

V526

A-PILLAR INNER LOWER RH

Sim Case ID:
Document Revision: 01
Area:
Robot:

Security class: Internal

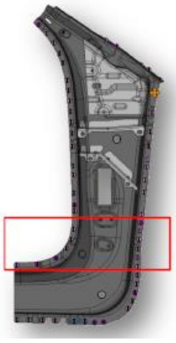

V526 A-PILLAR INNER LOWER

Joining Description
- Weld Point ID
- Location
- Number of parts in joint

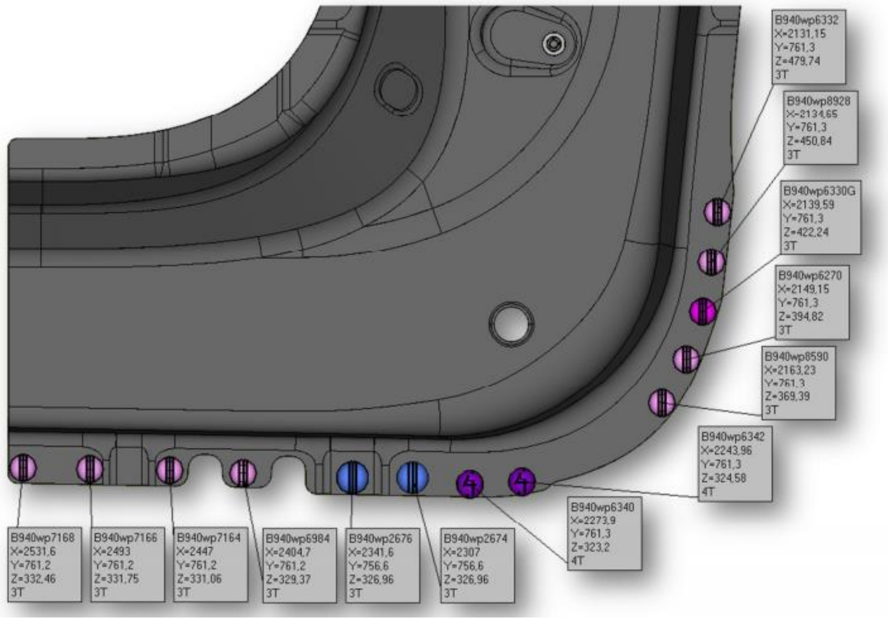

V526
A-PILLAR INNER LOWER RH

Sim Case ID:
Document Revision: 01
Area:
Robot:

Security class: Internal

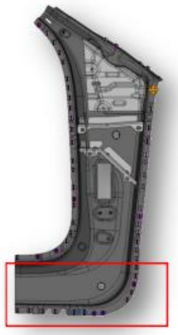

Appendix III: Results of the temperature vs. hardness test

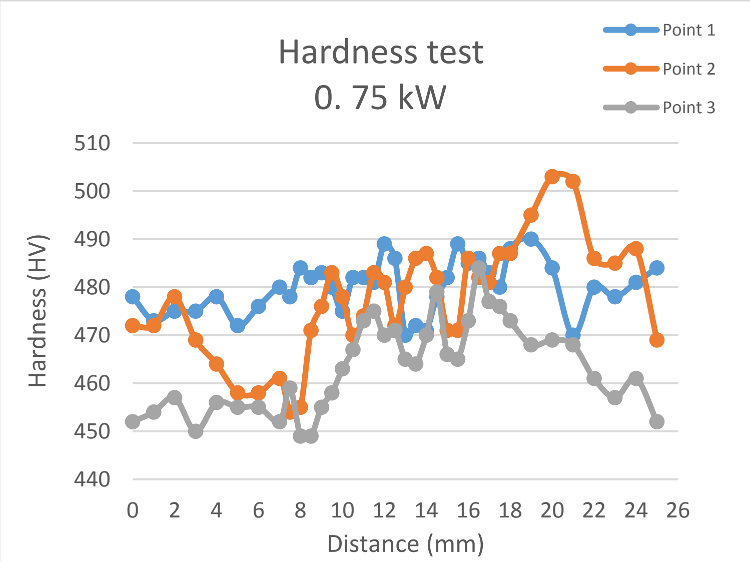

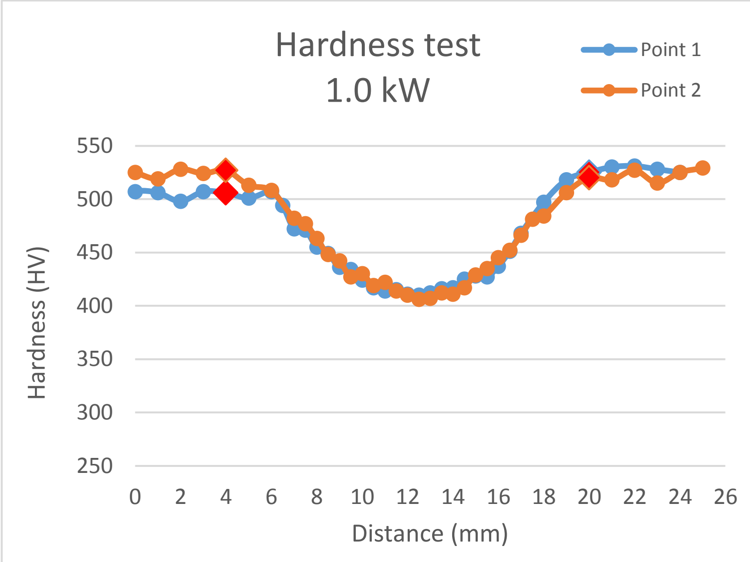

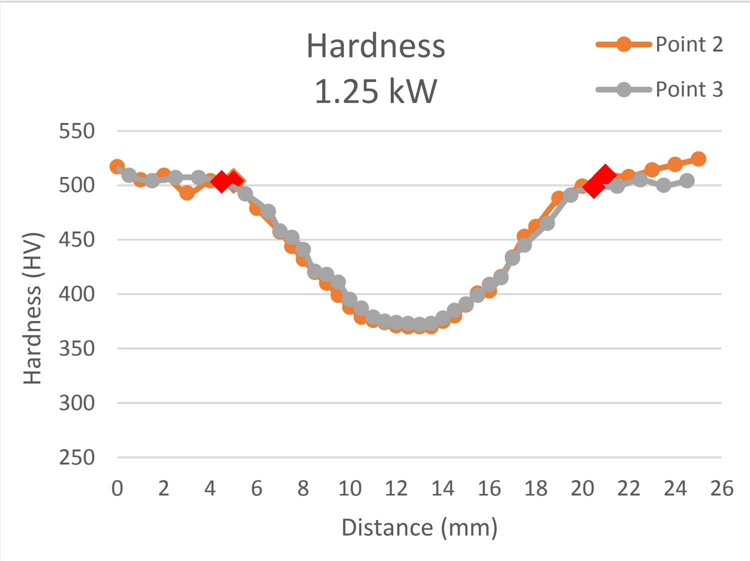

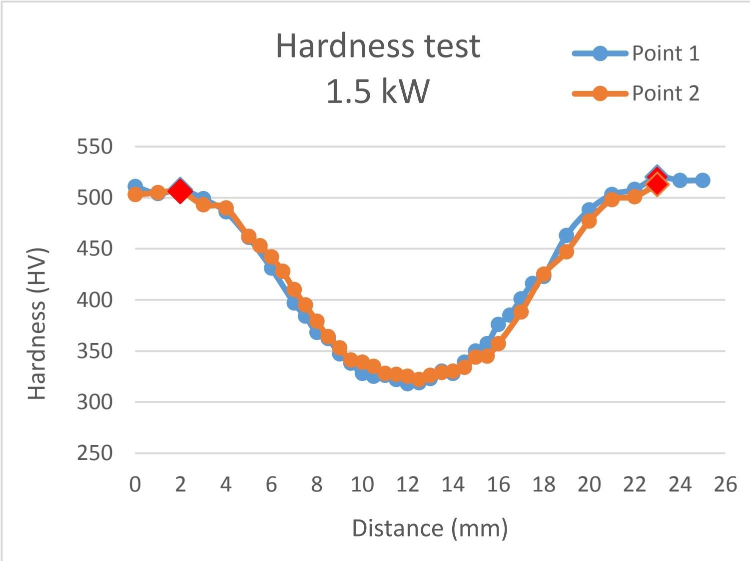

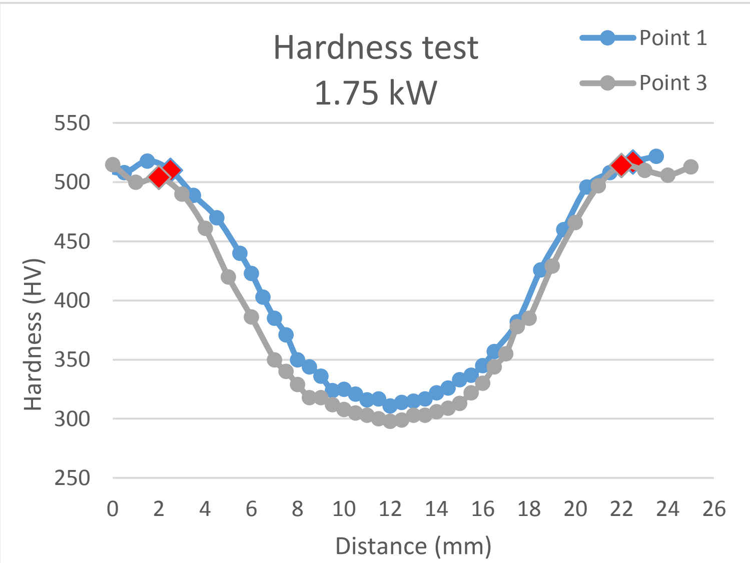

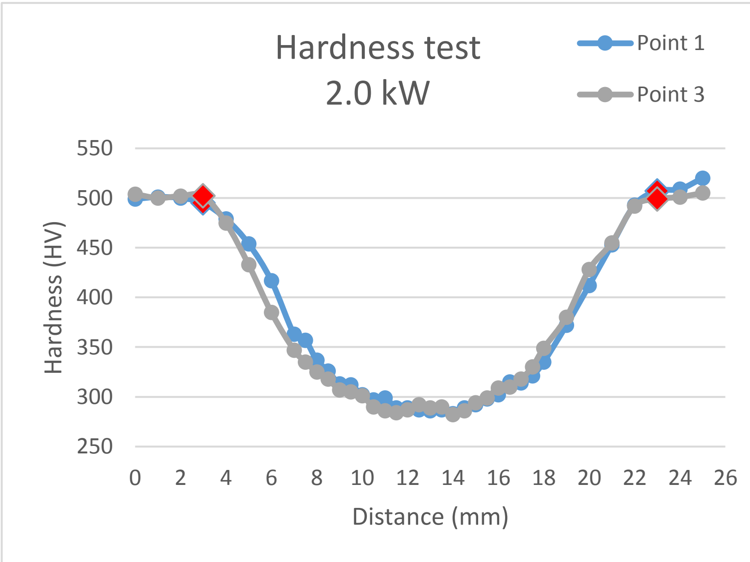

Measuring hardness from front side to the bottom side. Each line at the graph represent each line the figure. Top line is the front side of the coupon and the last line is the back side.

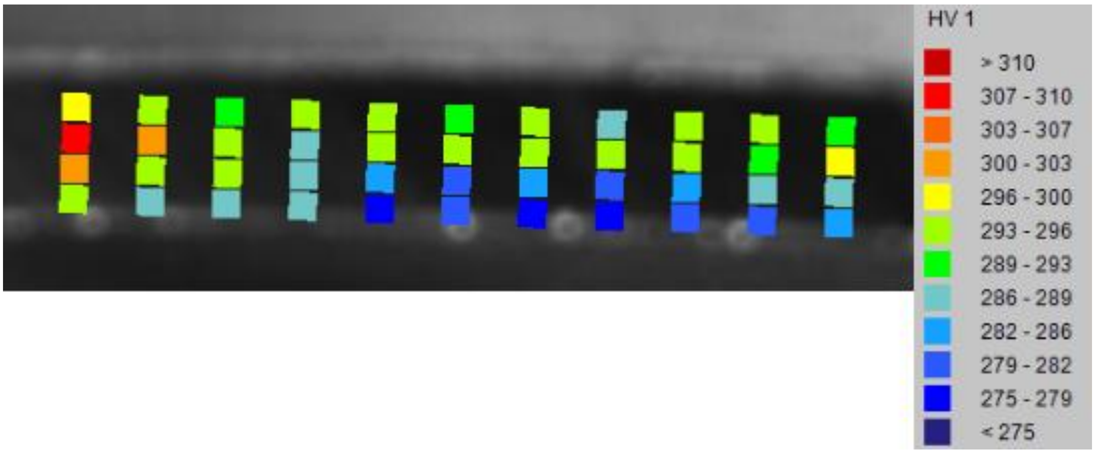

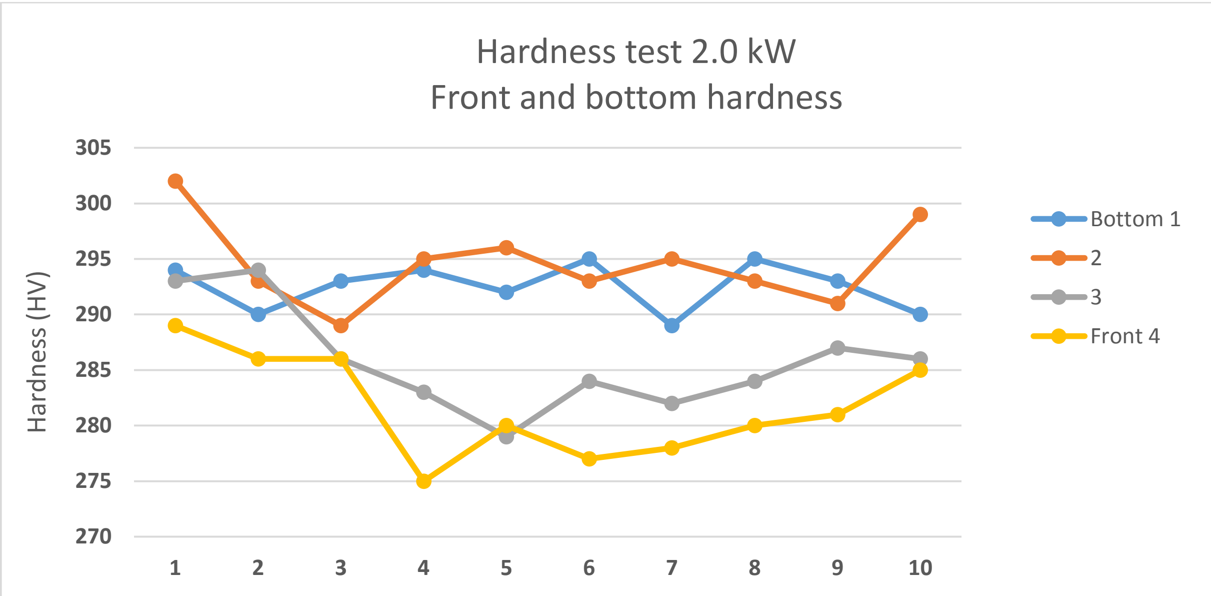

Appendix IV: RD&T sequences

Sequence A

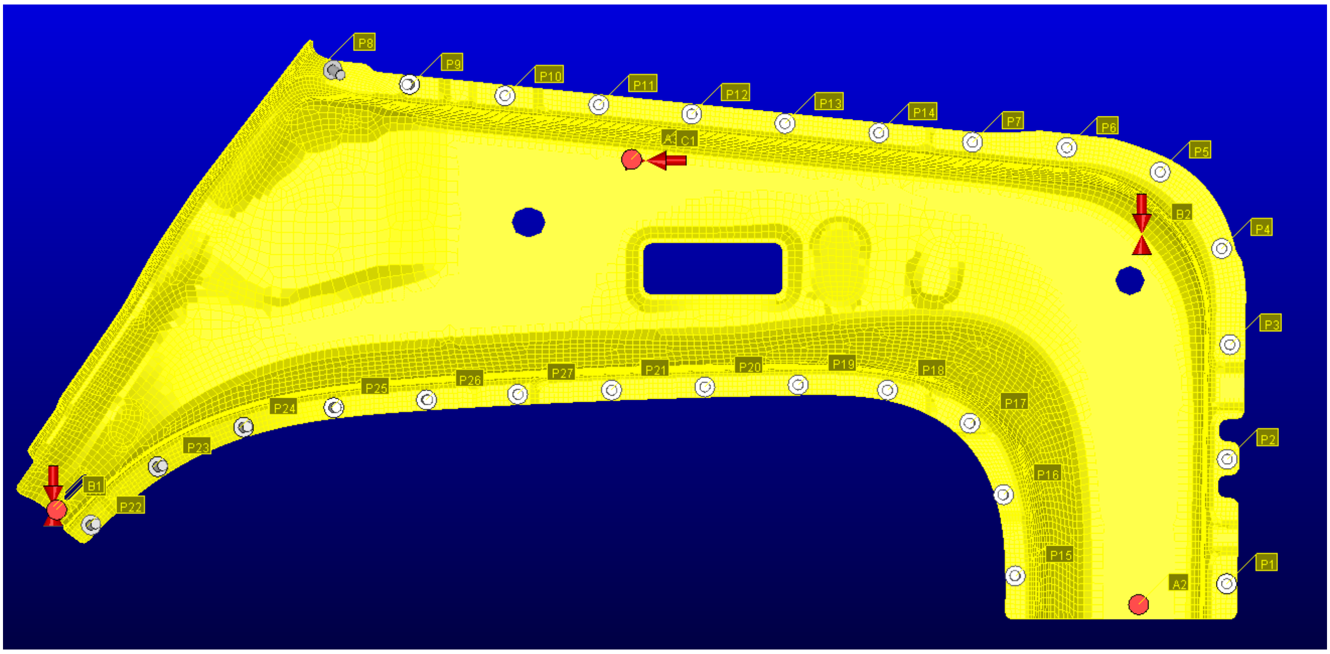

Sequence B

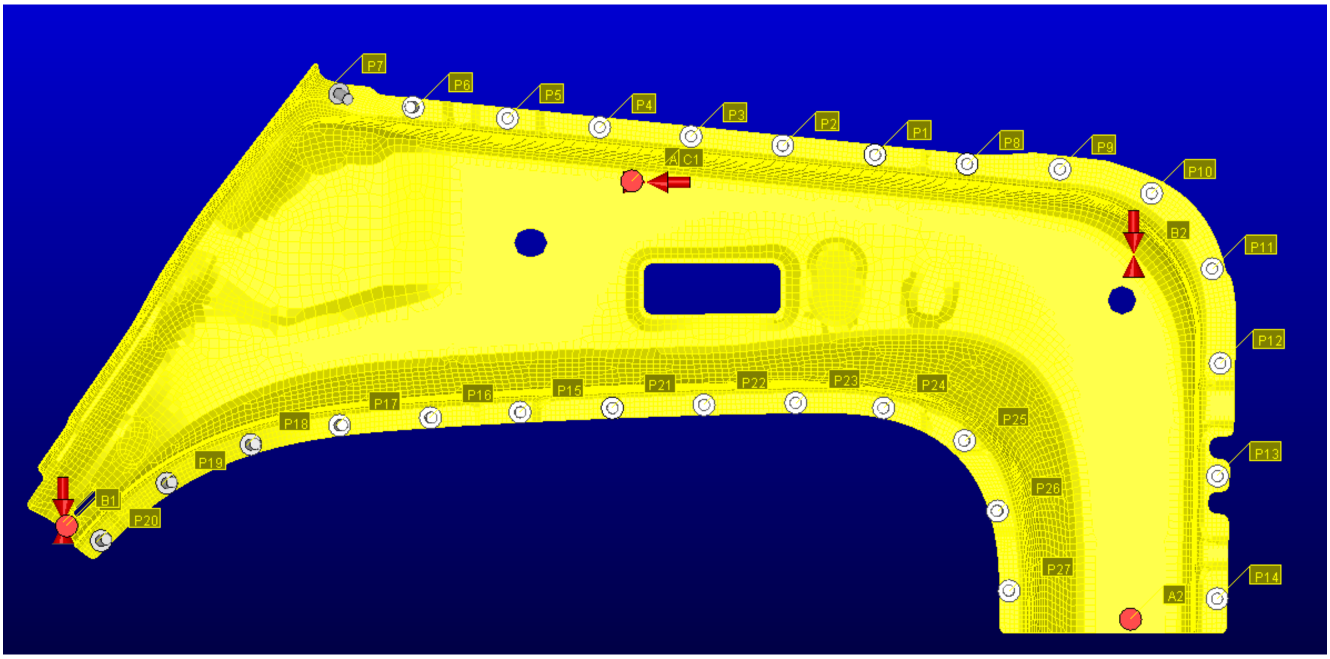

Sequence C

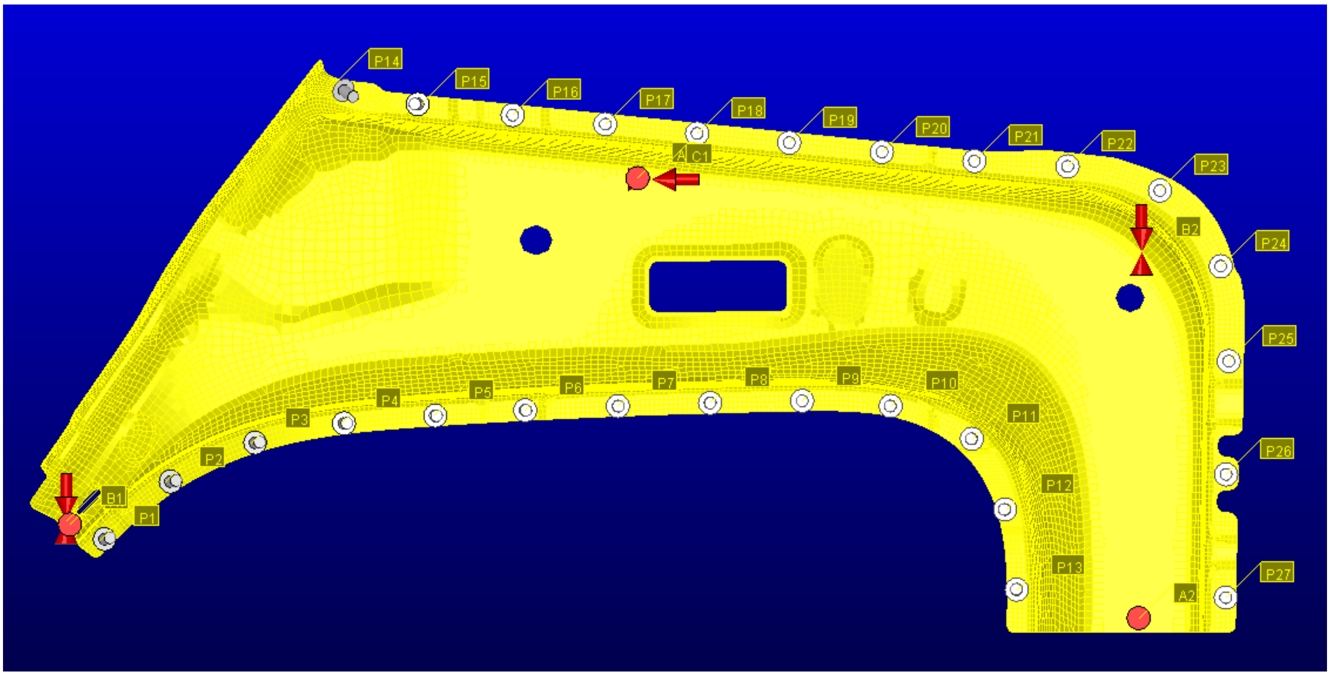

Sequence D

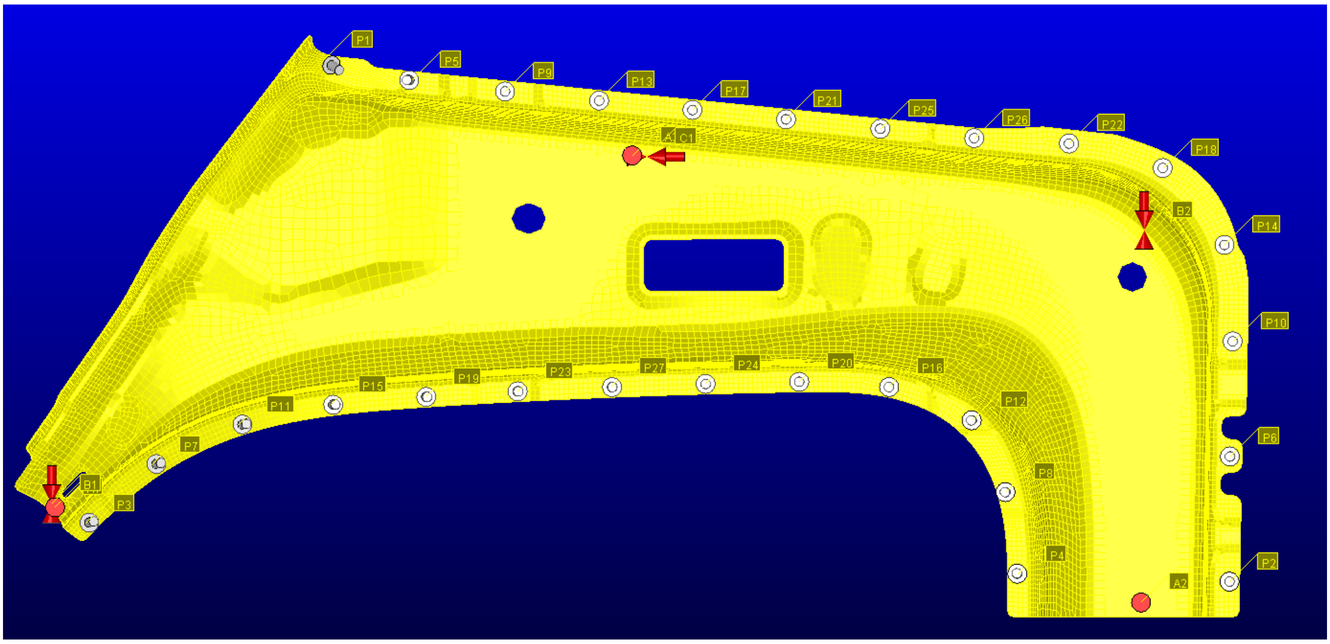

Sequence E

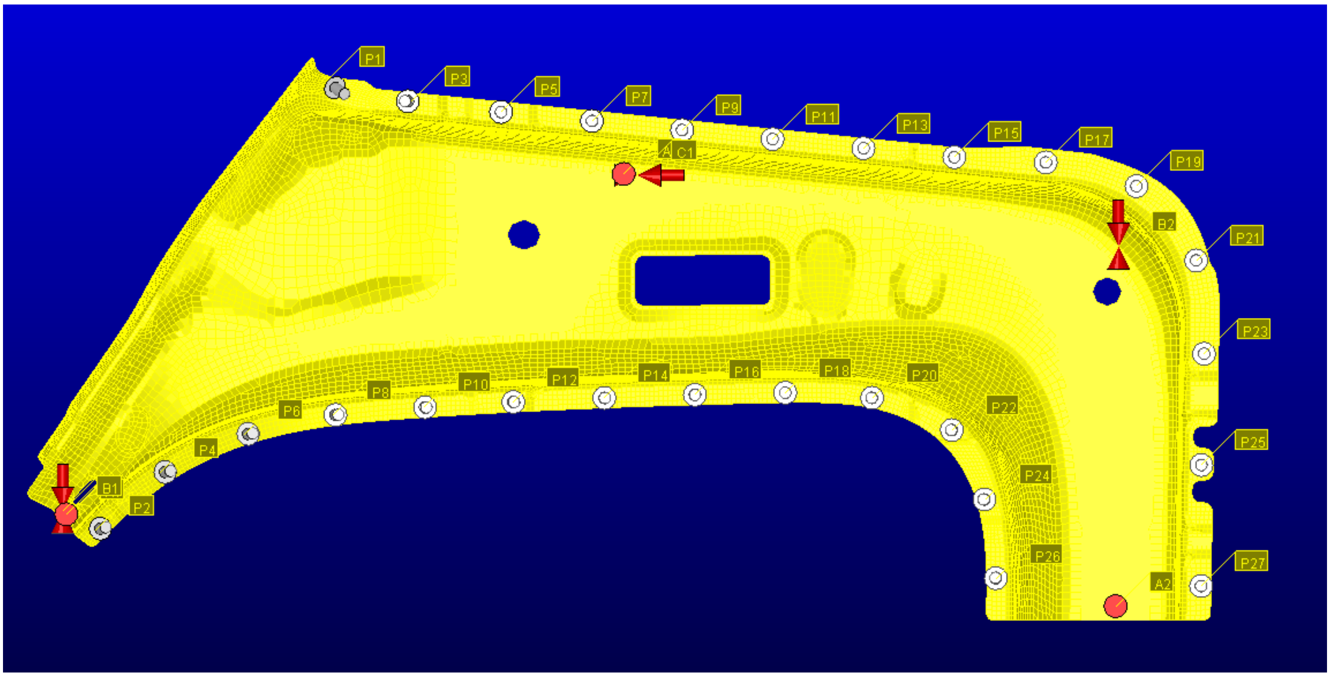

P1
P3
P5
P7
P9
P11
P13
P15
P17
P19
C1
B2
P21
P23
P25
P27
A2
P26
P24
P22
P20
P18
P16
P14
P12
P10
P8
P6
P4
B1
P2

Appendix V: Material data for Simulation.

```
*MATERIAL,
NAME=USIBOR_15
00
*UNITS,
SET=mmNS
*EXPANSION,
TYPE=ISO,
ZERO=25
1.531915e-05,
1.200000e+03
1.469388e-05,
1.250000e+03
1.411765e-05,
1.300000e+03
1.358491e-05,
1.350000e+03
1.309091e-05,
1.400000e+03
1.263158e-05,
1.450000e+03
1.220339e-05,
1.500000e+03
1.180328e-05,
1.550000e+03
1.142857e-05,
1.600000e+03
1.107692e-05,
1.650000e+03
1.074627e-05,
1.700000e+03
1.043478e-05,
1.750000e+03
1.014085e-05,
1.800000e+03
9.863014e-06,
1.850000e+03
9.600000e-06,
1.900000e+03
9.350649e-06,
1.950000e+03
9.113924e-06,
2.000000e+03
8.888889e-06,
2.050000e+03
8.674699e-06,
2.100000e+03
8.470588e-06,
2.150000e+03
8.275862e-06,
2.200000e+03
8.089888e-06,
2.250000e+03
7.912088e-06,
2.300000e+03
7.741935e-06,
2.350000e+03
7.578947e-06,
2.400000e+03
7.422680e-06,
2.450000e+03
7.272727e-06,
2.500000e+03
7.128713e-06,
2.550000e+03
6.990291e-06,
2.600000e+03
6.857143e-06,
2.650000e+03
6.728972e-06,
2.700000e+03
6.605505e-06,
2.750000e+03
6.486486e-06,
2.800000e+03
6.371681e-06,
2.850000e+03
6.260870e-06,
2.900000e+03
6.153846e-06,
2.950000e+03
6.050420e-06,
3.000000e+03
5.950413e-06,
3.050000e+03
5.853659e-06,
3.100000e+03
5.760000e-06,
3.150000e+03
5.669291e-06,
3.200000e+03
5.581395e-06,
3.250000e+03
5.496183e-06,
3.300000e+03
5.413534e-06,
3.350000e+03
5.333333e-06,
3.400000e+03
5.255474e-06,
3.450000e+03
5.179856e-06,
3.500000e+03
5.106383e-06,
3.550000e+03
5.034965e-06,
3.600000e+03
4.965517e-06,
3.650000e+03
4.897959e-06,
3.700000e+03
4.832215e-06,
3.750000e+03
4.768212e-06,
3.800000e+03
4.705882e-06,
3.850000e+03
4.645161e-06,
3.900000e+03
4.585987e-06,
3.950000e+03
4.528302e-06,
4.000000e+03
4.472050e-06,
4.050000e+03
4.417178e-06,
4.100000e+03
4.363636e-06,
4.150000e+03
4.311377e-06,
4.200000e+03
4.260355e-06,
4.250000e+03
4.210526e-06,
4.300000e+03
4.161850e-06,
4.350000e+03
4.114286e-06,
4.400000e+03
4.067797e-06,
4.450000e+03
4.022346e-06,
4.500000e+03
3.977901e-06,
4.550000e+03
3.934426e-06,
4.600000e+03
3.891892e-06,
4.650000e+03
3.850267e-06,
4.700000e+03
3.809524e-06,
4.750000e+03
3.769634e-06,
4.800000e+03
3.730570e-06,
4.850000e+03
3.692308e-06,
4.900000e+03
3.654822e-06,
4.950000e+03
3.618090e-06,
5.000000e+03
3.582090e-06,
5.050000e+03
3.546798e-06,
5.100000e+03
3.512195e-06,
5.150000e+03
3.478261e-06,
5.200000e+03
3.444976e-06,
5.250000e+03
3.412322e-06,
5.300000e+03
3.380282e-06,
5.350000e+03
3.348837e-06,
5.400000e+03
3.317972e-06,
5.450000e+03
3.287671e-06,
5.500000e+03
3.257919e-06,
5.550000e+03
3.228700e-06,
5.600000e+03
3.200000e-06,
5.650000e+03
3.171806e-06,
5.700000e+03
3.144105e-06,
5.750000e+03
3.116883e-06,
5.800000e+03
3.090129e-06,
5.850000e+03
3.063830e-06,
5.900000e+03
3.037975e-06,
5.950000e+03
3.012552e-06,
6.000000e+03
2.987552e-06,
6.050000e+03
2.962963e-06,
6.100000e+03
2.938776e-06,
6.150000e+03
2.914980e-06,
6.200000e+03
2.891566e-06,
6.250000e+03
2.868526e-06,
6.300000e+03
2.845850e-06,
6.350000e+03
2.823529e-06,
6.400000e+03
2.801556e-06,
6.450000e+03
2.779923e-06,
6.500000e+03
2.758621e-06,
6.550000e+03
2.737643e-06,
6.600000e+03
2.716981e-06,
6.650000e+03
2.696629e-06,
6.700000e+03
2.676580e-06,
6.750000e+03
```

```
2.656827e-06,
6.800000e+03
2.637363e-06,
6.850000e+03
2.618182e-06,
6.900000e+03
2.599278e-06,
6.950000e+03
2.580645e-06,
7.000000e+03
2.562278e-06,
7.050000e+03
2.544170e-06,
7.100000e+03
2.526316e-06,
7.150000e+03
2.508711e-06,
7.200000e+03
2.491349e-06,
7.250000e+03
2.474227e-06,
7.300000e+03
2.457338e-06,
7.350000e+03
2.440678e-06,
7.400000e+03
2.424242e-06,
7.450000e+03
2.408027e-06,
7.500000e+03
2.392027e-06,
7.550000e+03
2.376238e-06,
7.600000e+03
2.360656e-06,
7.650000e+03
2.345277e-06,
7.700000e+03
2.330097e-06,
7.750000e+03
2.315113e-06,
7.800000e+03
2.300319e-06,
7.850000e+03
2.285714e-06,
7.900000e+03
2.271293e-06,
7.950000e+03
2.257053e-06,
8.000000e+03
2.242991e-06,
8.050000e+03
2.229102e-06,
8.100000e+03
2.215385e-06,
8.150000e+03
2.201835e-06,
8.200000e+03
2.188450e-06,
8.250000e+03
2.175227e-06,
8.300000e+03
2.162162e-06,
8.350000e+03
2.149254e-06,
8.400000e+03
2.136499e-06,
8.450000e+03
2.123894e-06,
8.500000e+03
2.111437e-06,
8.550000e+03
2.099125e-06,
8.600000e+03
2.086957e-06,
8.650000e+03
2.074928e-06,
8.700000e+03
2.063037e-06,
8.750000e+03
2.051282e-06,
8.800000e+03
2.039660e-06,
8.850000e+03
2.028169e-06,
8.900000e+03
2.016807e-06,
8.950000e+03
2.005571e-06,
9.000000e+03
1.994460e-06,
9.050000e+03
1.983471e-06,
9.100000e+03
1.972603e-06,
9.150000e+03
1.961853e-06,
9.200000e+03
1.951220e-06,
9.250000e+03
1.940701e-06,
9.300000e+03
1.930295e-06,
9.350000e+03
1.920000e-06,
9.400000e+03
1.909814e-06,
9.450000e+03
1.899736e-06,
9.500000e+03
1.889764e-06,
9.550000e+03
1.879896e-06,
9.600000e+03
1.870130e-06,
9.650000e+03
1.860465e-06,
9.700000e+03
1.850900e-06,
9.750000e+03
1.841432e-06,
9.800000e+03
1.832061e-06,
9.850000e+03
1.822785e-06,
9.900000e+03
1.813602e-06,
9.950000e+03
1.804511e-06,
1.000000e+04
*ELASTIC,
TYPE=ISOTROPIC
207.883e+03,
0.29, 25.0
204.534e+03,
0.29, 100.0
198.502e+03,
0.3, 200.0
188.85e+03,
0.3, 300.0
166.137e+03,
0.31, 400.0
154.217e+03,
0.32, 500.0
144.477e+03,
0.33, 600.0
134.812e+03,
0.33, 700.0
125.151e+03,
0.34, 800.0
115.367e+03,
0.35, 900.0
113.395e+03,
0.35, 920.0
112.407e+03,
0.35, 930.0
*CONDUCTIVITY,
TYPE=ISO
38.09, 25.0
39.45, 100.0
39.81, 200.0
36.7, 300.0
23.38, 400.0
22.94, 500.0
23.93, 600.0
25.03, 700.0
26.2, 800.0
27.37, 900.0
27.6, 920.0
27.72, 930.0
*SPECIFIC HEAT
4.50372e+08,
25.0
4.85475e+08,
100.0
5.57182e+08,
200.0
8.4091e+08,
300.0
26.57616e+08,
400.0
5.72855e+08,
500.0
5.83981e+08,
600.0
5.83997e+08,
700.0
5.97236e+08,
800.0
6.12464e+08,
900.0
6.15569e+08,
920.0
6.14901e+08,
930.0
*DENSITY
7.790179e-09,
25.0
7.767847e-09,
100.0
7.7388e-09,
200.0
7.72325e-09,
300.0
7.814596e-09,
400.0
7.782508e-09,
500.0
7.72841e-09,
600.0
7.673319e-09,
700.0
7.617593e-09,
800.0
7.562355e-09,
900.0
7.551371e-09,
920.0
7.545882e-09,
930.0
*PLASTIC,
HARDENING=ISOT
ROPIC
1236.52, 0,
25.0
1514.4479,
0.02, 25.0
1609.7595,
0.04, 25.0
1668.2702,
0.06, 25.0
1711.0695,
0.08, 25.0
1745.0219,
0.1, 25.0
1773.2626,
0.12, 25.0
1797.496,
0.14, 25.0
1818.7555,
0.16, 25.0
```

1837.7162,
0.18, 25.0
1854.8447,
0.2, 25.0
1870.4767,
0.22, 25.0
1884.8626,
0.24, 25.0
1898.1941,
0.26, 25.0
1910.6212,
0.28, 25.0
1922.2636,
0.3, 25.0
1933.2186,
0.32, 25.0
1943.5661,
0.34, 25.0
1953.3727,
0.36, 25.0
1962.6944,
0.38, 25.0
1971.5791,
0.4, 25.0
1980.0675,
0.42, 25.0
1988.1949,
0.44, 25.0
1995.9922,
0.46, 25.0
2003.4862,
0.48, 25.0
2010.7007,
0.5, 25.0
2043.241, 0.6,
25.0
2071.164, 0.7,
25.0
2095.6602,
0.8, 25.0
2117.5077,
0.9, 25.0
2137.2439, 1,
25.0
1069.3, 0,
100.0
1333.0039,
0.02, 100.0
1424.4578,
0.04, 100.0
1480.8366,
0.06, 100.0
1522.1861,
0.08, 100.0
1555.0528,
0.1, 100.0
1582.4329,
0.12, 100.0
1605.9582,
0.14, 100.0
1626.6193,
0.16, 100.0
1645.0642,
0.18, 100.0
1661.7408,
0.2, 100.0
1676.9723,
0.22, 100.0
1690.9994,
0.24, 100.0
1704.0067,
0.26, 100.0
1716.1388,
0.28, 100.0
1727.5111,
0.3, 100.0
1738.2173,
0.32, 100.0
1748.3348,
0.34, 100.0
1757.9277,
0.36, 100.0
1767.0502,
0.38, 100.0
1775.7485,
0.4, 100.0
1784.062,
0.42, 100.0
1792.025,
0.44, 100.0
1799.6671,
0.46, 100.0
1807.0144,
0.48, 100.0
1814.09, 0.5,
100.0
1846.031, 0.6,
100.0
1873.4752,
0.7, 100.0
1897.5779,
0.8, 100.0
1919.0953,
0.9, 100.0
1938.5499, 1,
100.0
953.069, 0,
200.0
1203.8837,
0.02, 200.0
1291.5973,
0.04, 200.0
1345.8398,
0.06, 200.0
1385.7015,
0.08, 200.0
1417.4319,
0.1, 200.0
1443.8961,
0.12, 200.0
1466.6564,
0.14, 200.0
1486.662,
0.16, 200.0
1504.5347,
0.18, 200.0
1520.7043,
0.2, 200.0
1535.4811,
0.22, 200.0
1549.0966,
0.24, 200.0
1561.7283,
0.26, 200.0
1573.5152,
0.28, 200.0
1584.5685,
0.3, 200.0
1594.9784,
0.32, 200.0
1604.8194,
0.34, 200.0
1614.1532,
0.36, 200.0
1623.0323,
0.38, 200.0
1631.5009,
0.4, 200.0
1639.5973,
0.42, 200.0
1647.3544,
0.44, 200.0
1654.8009,
0.46, 200.0
1661.9619,
0.48, 200.0
1668.8597,
0.5, 200.0
1700.0182,
0.6, 200.0
1726.8158,
0.7, 200.0
1750.3701,
0.8, 200.0
1771.413, 0.9,
200.0
1790.4508, 1,
200.0
887.499, 0,
300.0
1129.8208,
0.02, 300.0
1214.9827,
0.04, 300.0
1267.7447,
0.06, 300.0
1306.5637,
0.08, 300.0
1337.4908,
0.1, 300.0
1363.3027,
0.12, 300.0
1385.5146,
0.14, 300.0
1405.0477,
0.16, 300.0
1422.5056,
0.18, 300.0
1438.306, 0.2,
300.0
1452.7503,
0.22, 300.0
1466.0635,
0.24, 300.0
1478.4182,
0.26, 300.0
1489.9497,
0.28, 300.0
1500.7661,
0.3, 300.0
1510.9552,
0.32, 300.0
1520.5894,
0.34, 300.0
1529.729,
0.36, 300.0
1538.4249,
0.38, 300.0
1546.7203,
0.4, 300.0
1554.6524,
0.42, 300.0
1562.2534,
0.44, 300.0
1569.5511,
0.46, 300.0
1576.5701,
0.48, 300.0
1583.332, 0.5,
300.0
1613.8884,
0.6, 300.0
1640.183, 0.7,
300.0
1663.3065,
0.8, 300.0
1683.9733,
0.9, 300.0
1702.6779, 1,
300.0
845.63, 0,
400.0
1082.0318,
0.02, 400.0
1165.3817,
0.04, 400.0
1217.0838,
0.06, 400.0
1255.1521,
0.08, 400.0

1285.4983,
0.1, 400.0
1310.8368,
0.12, 400.0
1332.6495,
0.14, 400.0
1351.8376,
0.16, 400.0
1368.992,
0.18, 400.0
1384.5214,
0.2, 400.0
1398.7213,
0.22, 400.0
1411.8118,
0.24, 400.0
1423.9621,
0.26, 400.0
1435.3047,
0.28, 400.0
1445.9456,
0.3, 400.0
1455.9709,
0.32, 400.0
1465.4516,
0.34, 400.0
1474.4467,
0.36, 400.0
1483.0061,
0.38, 400.0
1491.1724,
0.4, 400.0
1498.9818,
0.42, 400.0
1506.466,
0.44, 400.0
1513.6524,
0.46, 400.0
1520.5649,
0.48, 400.0
1527.2249,
0.5, 400.0
1557.3281,
0.6, 400.0
1583.2424,
0.7, 400.0
1606.0388,
0.8, 400.0
1626.4188,
0.9, 400.0
1644.8685, 1,
400.0
816.658, 0,
500.0
1031.4943,
0.02, 500.0
1098.5004,
0.04, 500.0
1096.5206,
0.06, 500.0
1092.3032,
0.08, 500.0
1086.1444,
0.1, 500.0
1078.9585,
0.12, 500.0
1071.4842,
0.14, 500.0
1064.1409,
0.16, 500.0
1057.1084,
0.18, 500.0
1050.4548,
0.2, 500.0
1044.1946,
0.22, 500.0
1038.3086,
0.24, 500.0
1032.7759,
0.26, 500.0
1027.5647,
0.28, 500.0
1022.6519,
0.3, 500.0
1018.0102,
0.32, 500.0
1013.6072,
0.34, 500.0
1009.4317,
0.36, 500.0
1005.461,
0.38, 500.0
1001.6775,
0.4, 500.0
998.0684,
0.42, 500.0
994.6101,
0.44, 500.0
991.3018,
0.46, 500.0
988.1296,
0.48, 500.0
985.0816, 0.5,
500.0
971.4224, 0.6,
500.0
959.8635, 0.7,
500.0
949.8591, 0.8,
500.0
941.0574, 0.9,
500.0
933.2037, 1,
500.0
421.2155, 0,
600.0
421.2035,
0.02, 600.0
421.0132,
0.04, 600.0
420.2517,
0.06, 600.0
418.6334,
0.08, 600.0
416.2721, 0.1,
600.0
413.515, 0.12,
600.0
410.6515,
0.14, 600.0
407.8396,
0.16, 600.0
405.1441,
0.18, 600.0
402.5896, 0.2,
600.0
400.1931,
0.22, 600.0
397.9427,
0.24, 600.0
395.8172,
0.26, 600.0
393.8205,
0.28, 600.0
391.9422, 0.3,
600.0
390.1571,
0.32, 600.0
388.4652,
0.34, 600.0
386.8723,
0.36, 600.0
385.3439,
0.38, 600.0
383.9014, 0.4,
600.0
382.5077,
0.42, 600.0
381.189, 0.44,
600.0
379.9258,
0.46, 600.0
378.7013,
0.48, 600.0
377.5302, 0.5,
600.0
372.2984, 0.6,
600.0
367.8733, 0.7,
600.0
364.0429, 0.8,
600.0
360.6577, 0.9,
600.0
357.6483, 1,
600.0
152.3919, 0,
700.0
152.3875,
0.02, 700.0
152.3181,
0.04, 700.0
152.0491,
0.06, 700.0
151.4513,
0.08, 700.0
150.5936, 0.1,
700.0
149.5936,
0.12, 700.0
148.554, 0.14,
700.0
147.533, 0.16,
700.0
146.5564,
0.18, 700.0
145.6352, 0.2,
700.0
144.7737,
0.22, 700.0
143.9767,
0.24, 700.0
143.1895,
0.26, 700.0
142.4544,
0.28, 700.0
141.7857, 0.3,
700.0
141.1448,
0.32, 700.0
140.5176,
0.34, 700.0
139.9717,
0.36, 700.0
139.388, 0.38,
700.0
138.8859, 0.4,
700.0
138.3625,
0.42, 700.0
137.9083,
0.44, 700.0
137.4224,
0.46, 700.0
137.0181,
0.48, 700.0
136.5597, 0.5,
700.0
134.6701, 0.6,
700.0
133.0871, 0.7,
700.0
131.6789, 0.8,
700.0
130.4506, 0.9,
700.0
129.3633, 1,
700.0
80.0205, 0,
800.0

80.0202, 0.02,
800.0
80.0125, 0.04,
800.0
79.9767, 0.06,
800.0
79.8822, 0.08,
800.0
79.7061, 0.1,
800.0
79.451, 0.12,
800.0
79.151, 0.14,
800.0
78.7956, 0.16,
800.0
78.4023, 0.18,
800.0
78.0558, 0.2,
800.0
77.6469, 0.22,
800.0
77.2771, 0.24,
800.0
76.9611, 0.26,
800.0
76.5701, 0.28,
800.0
76.2475, 0.3,
800.0
75.9756, 0.32,
800.0
75.622, 0.34,
800.0
75.3281, 0.36,
800.0
75.0856, 0.38,
800.0
74.8058, 0.4,
800.0
74.5204, 0.42,
800.0
74.2802, 0.44,
800.0
74.0782, 0.46,
800.0
73.8404, 0.48,
800.0
73.5878, 0.5,
800.0
72.5888, 0.6,
800.0
71.7524, 0.7,
800.0
71.0426, 0.8,
800.0
70.3276, 0.9,
800.0
69.7589, 1,
800.0
58.5242, 0,
900.0
66.8757, 0.02,
900.0
66.8732, 0.04,
900.0
66.8617, 0.06,
900.0
66.8314, 0.08,
900.0
66.7686, 0.1,
900.0
66.6629, 0.12,
900.0
66.5094, 0.14,
900.0
66.3136, 0.16,
900.0
66.0909, 0.18,
900.0
65.8193, 0.2,
900.0
65.516, 0.22,
900.0
65.2252, 0.24,
900.0
64.9452, 0.26,
900.0
64.6099, 0.28,
900.0
64.3095, 0.3,
900.0
64.0474, 0.32,
900.0
63.7345, 0.34,
900.0
63.4396, 0.36,
900.0
63.1843, 0.38,
900.0
62.9467, 0.4,
900.0
62.6537, 0.42,
900.0
62.3982, 0.44,
900.0
62.1769, 0.46,
900.0
61.9776, 0.48,
900.0
61.7127, 0.5,
900.0
60.6816, 0.6,
900.0
59.8088, 0.7,
900.0
59.0511, 0.8,
900.0
58.3137, 0.9,
900.0
57.7034, 1,
900.0
40.2216, 0,
1000.0
40.2216, 0.02,
1000.0
40.2202, 0.04,
1000.0
40.2135, 0.06,
1000.0
40.196, 0.08,
1000.0
40.1605, 0.1,
1000.0
40.1026, 0.12,
1000.0
40.0223, 0.14,
1000.0
39.8954, 0.16,
1000.0
39.7337, 0.18,
1000.0
39.5568, 0.2,
1000.0
39.3779, 0.22,
1000.0
39.2089, 0.24,
1000.0
39.0576, 0.26,
1000.0
38.8665, 0.28,
1000.0
38.651, 0.3,
1000.0
38.4581, 0.32,
1000.0
38.29, 0.34,
1000.0
38.1457, 0.36,
1000.0
38.0234, 0.38,
1000.0
37.8343, 0.4,
1000.0
37.646, 0.42,
1000.0
37.4813, 0.44,
1000.0
37.3381, 0.46,
1000.0
37.2141, 0.48,
1000.0
37.1072, 0.5,
1000.0
36.4351, 0.6,
1000.0
36.0021, 0.7,
1000.0
35.4261, 0.8,
1000.0
35.0776, 0.9,
1000.0
34.6553, 1,
1000.0
25.0093, 0,
1100.0
25.0093, 0.02,
1100.0
25.0085, 0.04,
1100.0
25.0049, 0.06,
1100.0
24.9941, 0.08,
1100.0
24.9681, 0.1,
1100.0
24.9232, 0.12,
1100.0
24.8558, 0.14,
1100.0
24.7656, 0.16,
1100.0
24.657, 0.18,
1100.0
24.5378, 0.2,
1100.0
24.417, 0.22,
1100.0
24.3027, 0.24,
1100.0
24.2, 0.26,
1100.0
24.1115, 0.28,
1100.0
24.0373, 0.3,
1100.0
23.9311, 0.32,
1100.0
23.7749, 0.34,
1100.0
23.6341, 0.36,
1100.0
23.5097, 0.38,
1100.0
23.401, 0.4,
1100.0
23.3071, 0.42,
1100.0
23.2266, 0.44,
1100.0
23.1577, 0.46,
1100.0
23.099, 0.48,
1100.0
23.049, 0.5,
1100.0
22.5686, 0.6,
1100.0
22.2302, 0.7,
1100.0

```
22.042, 0.8,
1100.0
21.7159, 0.9,
1100.0
21.4197, 1,
1100.0
15.9181, 0,
1200.0
15.9181, 0.02,
1200.0
15.9175, 0.04,
1200.0
15.9149, 0.06,
1200.0
15.9082, 0.08,
1200.0
15.894, 0.1,
1200.0
15.8696, 0.12,
1200.0
15.8342, 0.14,
1200.0
15.7883, 0.16,
1200.0
15.7318, 0.18,
1200.0
15.6687, 0.2,
1200.0
15.6019, 0.22,
1200.0
15.5299, 0.24,
1200.0
15.4577, 0.26,
1200.0
15.3867, 0.28,
1200.0
15.3153, 0.3,
1200.0
15.2443, 0.32,
1200.0
15.1766, 0.34,
1200.0
15.1106, 0.36,
1200.0
15.0447, 0.38,
1200.0
14.983, 0.4,
1200.0
14.9218, 0.42,
1200.0
14.8624, 0.44,
1200.0
14.8069, 0.46,
1200.0
14.7499, 0.48,
1200.0
14.6987, 0.5,
1200.0
14.4522, 0.6,
1200.0
14.2409, 0.7,
1200.0
14.0557, 0.8,
1200.0
13.8934, 0.9,
1200.0
13.7438, 1,
1200.0
10.2379, 0,
1300.0
10.2379, 0.02,
1300.0
10.2375, 0.04,
1300.0
10.2358, 0.06,
1300.0
10.2314, 0.08,
1300.0
10.2223, 0.1,
1300.0
10.2073, 0.12,
1300.0
10.1843, 0.14,
1300.0
10.1536, 0.16,
1300.0
10.1181, 0.18,
1300.0
10.0774, 0.2,
1300.0
10.033, 0.22,
1300.0
9.9887, 0.24,
1300.0
9.9407, 0.26,
1300.0
9.8969, 0.28,
1300.0
9.8484, 0.3,
1300.0
9.8056, 0.32,
1300.0
9.7594, 0.34,
1300.0
9.7176, 0.36,
1300.0
9.6757, 0.38,
1300.0
9.6345, 0.4,
1300.0
9.5985, 0.42,
1300.0
9.5573, 0.44,
1300.0
9.5215, 0.46,
1300.0
9.4871, 0.48,
1300.0
9.4504, 0.5,
1300.0
9.2968, 0.6,
1300.0
9.1574, 0.7,
1300.0
9.0381, 0.8,
1300.0
8.9325, 0.9,
1300.0
8.8374, 1,
1300.0
```

Appendix VI: Displacement plot of all the data points for each sequence

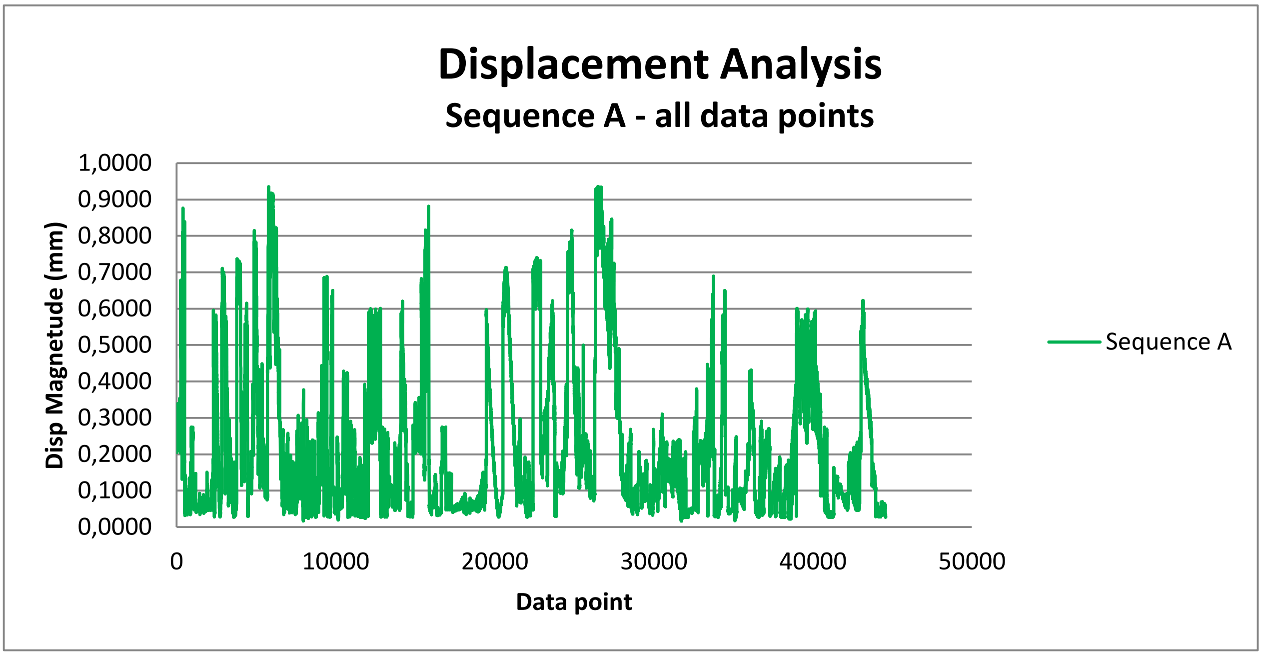

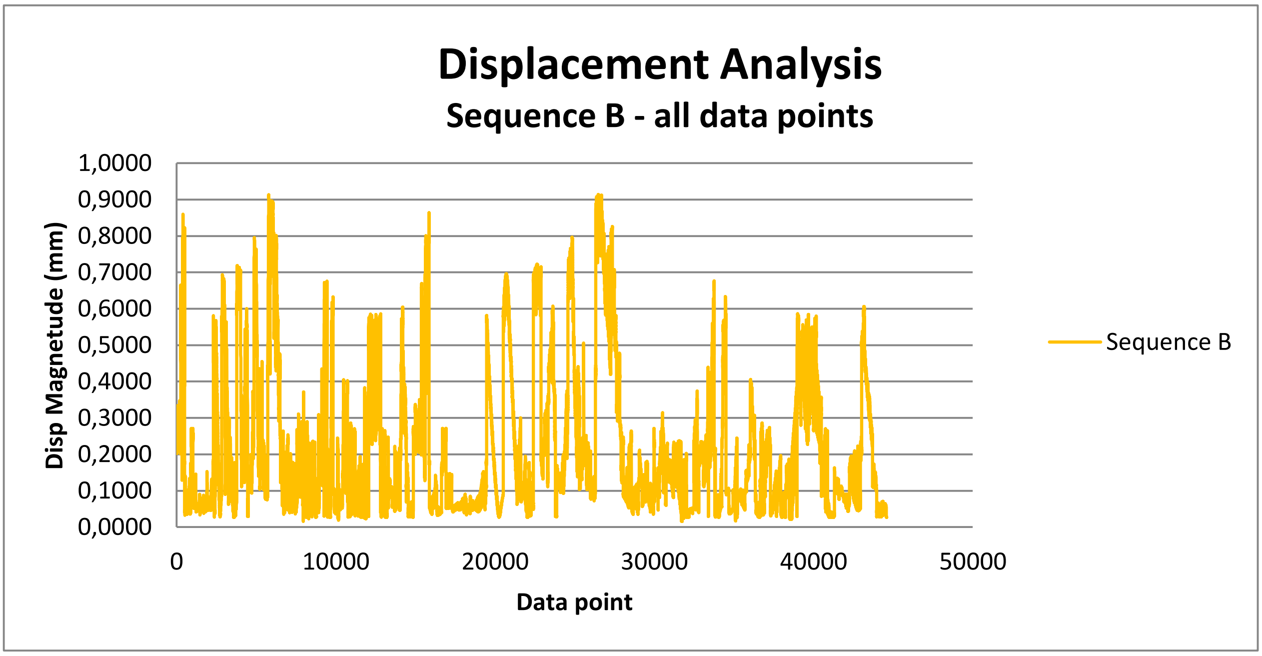

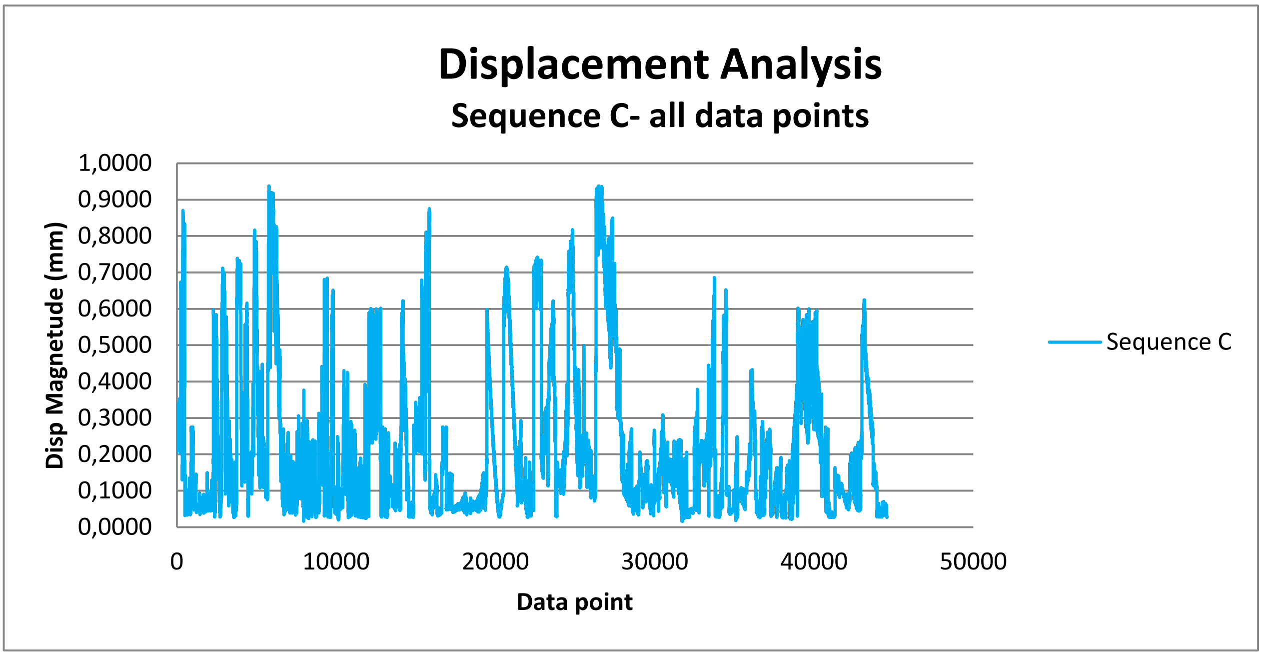
Displacement Analysis
Sequence C- all data points
1,0000
0,9000
0,8000
0,7000
0,6000
0,5000
0,4000
0,3000
0,2000
0,1000
0,0000
Disp Magnetude (mm)
0
10000
20000
30000
40000
50000
Data point
Sequence C

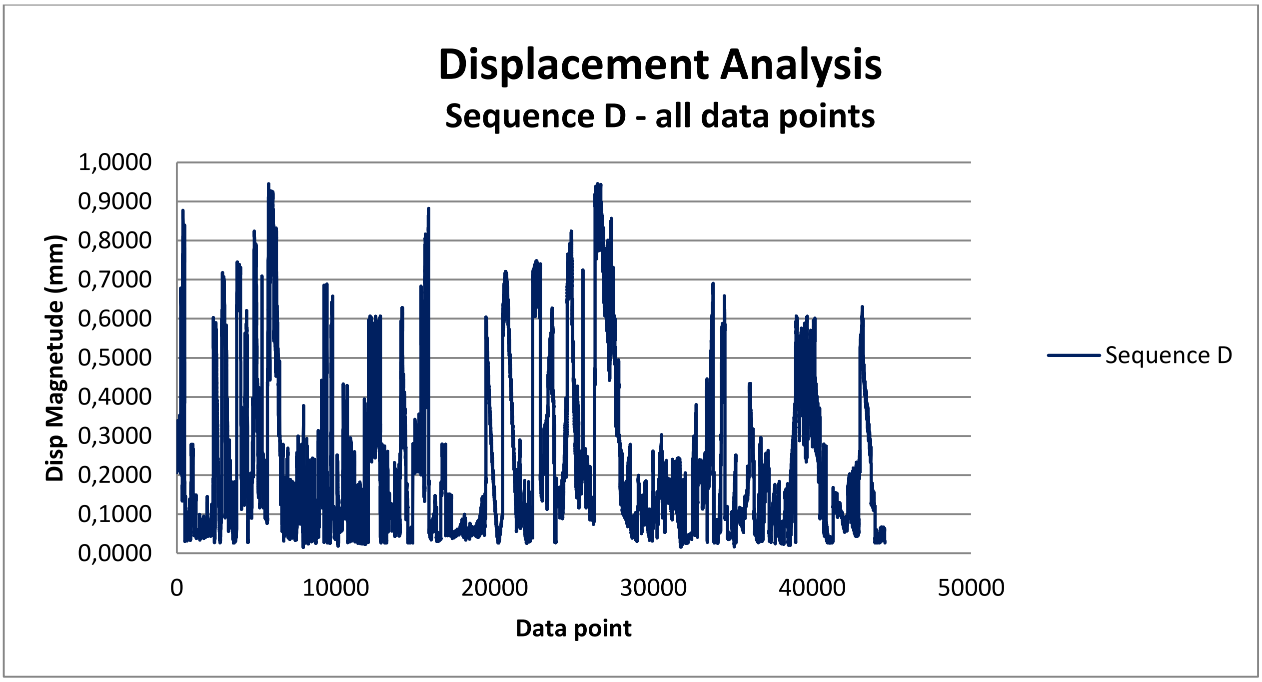
Displacement Analysis
Sequence D - all data points
1,0000
0,9000
0,8000
0,7000
0,6000
0,5000
0,4000
0,3000
0,2000
0,1000
0,0000
Disp Magnetude (mm)
0
10000
20000
30000
40000
50000
Data point
Sequence D

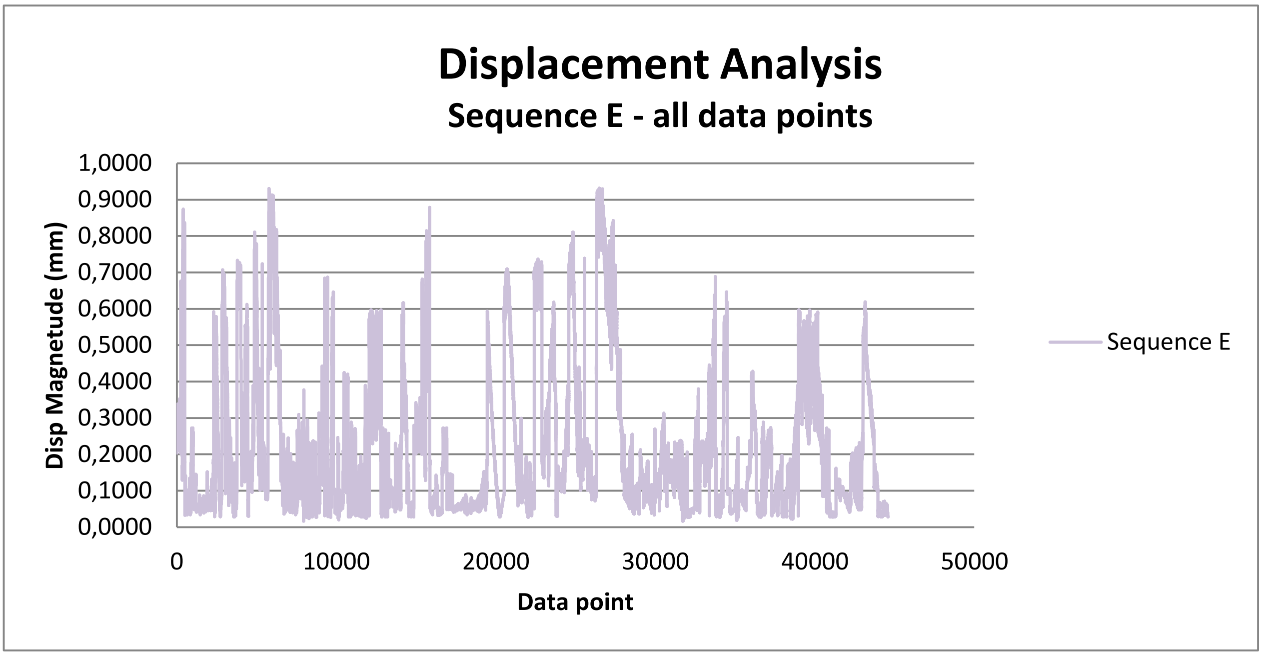
Displacement Analysis
Sequence E - all data points
Disp Magnetude (mm)
1,0000
0,9000
0,8000
0,7000
0,6000
0,5000
0,4000
0,3000
0,2000
0,1000
0,0000
0
10000
20000
30000
40000
50000
Data point
Sequence E

Appendix VII: Displacement plot of the line sample and statistical analysis